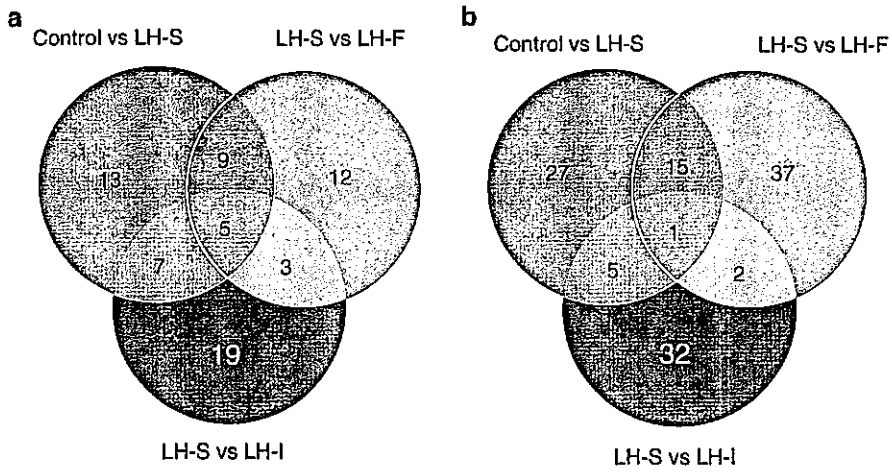

Figure 4 Venn-diagram selection of LH- and antidepressant-associated transcripts in the frontal cortex (a) and hippocampus (b). Comparisons were made between control ($n=6$) and LH-S rats ($n=6$), between LH-S and LH-F rats ($n=5$), and between LH-S and LH-I rats ($n=5$). The LH-I and LH-F rats were those that showed more than 50% success in escape behavior after drug treatments. The number in each compartment denotes the number of differentially expressed transcripts between two groups (see Materials and Methods for a definition of our criteria).

increased after initiating therapy. Approximately 38% of LH-associated transcripts in the FC and 56% in the HPC could not be normalized by either antidepressant (Figure 4; red area). These transcripts could represent the potential targets for novel antidepressants with efficacy against refractory depression. The green, purple and light blue segments in Figure 4 depict the transcripts with expression levels that did not differ between control and LH-S groups, but were significantly altered by fluoxetine, imipramine or both drug treatments, respectively. The information on these transcripts is provided as supplementary Tables S1 and S2. Some of these transcripts may be relevant to the manifestation of adverse reactions by TCA and SSRI. Tables 1 and 2 show the listing of LH-associated transcripts according to putative functions, along with *P*-values between different treatment groups. Data are also provided on the 'average difference'±SE of each transcript (that corresponds to an absolute value) in supplementary Tables S1 and S2. In all, 17 known genes and one EST showed downregulation (marked in red), whereas 16 transcripts including ESTs were upregulated in the FC (Table 1). In contrast, the majority of known LH-associated genes in the HPC were downregulated (27 of 31) (marked in red in Table 2). Even allowing for ESTs, the number of downregulated transcripts in the HPC significantly exceeds the upregulated transcripts (32 *vs* 16) (Table 2).

We chose four genes from each of Tables 1 and 2, and examined mRNA levels in the same RNA samples used for microarray experiments under 'one-step' quantitative RT-PCR reactions (Table 3). These results showed the same direction of expressional changes seen in the microarray experiments, but less correlation was found with the degree of change between the two methods, as indicated in prior studies.[25,26] Furthermore, since only a limited number of transcripts were confirmed by independent methods and no transcripts were confirmed when Bonferroni's correction was applied to the quantitative RT-PCR results, the present DNA microarray data are broadly unconfirmed.

LH-associated Transcripts in the FC

When classified according to function, genes defined as receptors or ion channel/transporters were all downregulated in LH animals (Table 1). Among them, the serotonin receptor type 2A (*Htr2a*) gene showed a 1.6-fold decrease, and recovery with both fluoxetine and imipramine. Evidence from other animal models for depression[27,28] and clinical observations[29] have also suggested a pathological role for *HTR2A* in the depressive state. The change in inositol-1,4,5-triphosphate receptor type 1 (*Itpr1*) level was small, but statistically significant. Both types of antidepressant normalized the reduced expression of *Itpr1*. The observed decrease in both *Htr2a* and *Itpr1* and their restitution to original levels by antidepressants is in keeping with a proposed theory of dysregulated monoamine-mediated calcium signaling in depression.[30,31] Other members of the receptor and ion channel/transporter gene families that showed restoration with fluoxetine or imipramine included a voltage-gated potassium channel and zinc transporter (Table 1). Conversely, three genes from the signal transduction family were all upregulated in LH-S rats compared to controls (Table 1). Of interest is prostaglandin D synthase, an enzyme that produces prostaglandin D_2, a potent endogenous sleep-promoting substance.[32] This enzyme has recently been implicated in the regulation of nonrapid eye movement (NREM).[33] Sleep disturbance is a typical symptom of human depression. Examination of sleep parameters in LH rats, particularly the NREM period, would therefore be of interest. Protein kinase C epsilon (PKCε), which is a member of nPKC, showed a small but significant increase in LH-S compared with controls.

Table 1 LH-associated transcripts in the frontal cortex

Functional Groups	*Fold change*[a]	*P-value*[b]			*Accession no.*
		Cont vs LH-S	*LH-S vs LH-F*	*LH-S vs LH-I*	
Receptor					
Inositol-1,4,5-triphosphate receptor type I	−1.1	0.0032	0.0078	0.0078	J05510
Serotonin receptor 2A	−1.6	0.0479	0.0352	0.0358	M64867
Ion channel/Transporter					
Voltage-gated potassium channel	−1.1	0.0289	0.0078		X62840
Dri 27/ZnT4 (zinc transporter)	−1.3	0.0289		0.0026	Y16774
Cl-/HCO3- exchanger (B3RP2)	−1.4	0.0484			J05166
Signal transduction					
Prostaglandin D2 synthetase	1.3	0.0484	0.0006	0.0181	J04488
PKC epsilon	1.2	0.0158	0.0181		M18331
Neurexophilin 4	2.0	0.0156			AF042714
Neural growth/ structure					
Tau	−1.1	0.0479	0.0358		X79321
Jagged2 precursor	1.3	0.0158		0.0358	U70050
Similar to cdc37	1.6	0.0484			D26564
MAP2	−1.4	0.0158			S74265
H36-alpha7 integrin alpha chain	−1.5	0.0289			X65036
Neu differentiation factor	−1.6	0.0484			M92430
LIMK-1	−9.5	0.0436			D31873
Metabolic enzymes					
Thioradoxin reductase 1	−1.2	0.0011	0.0181		AA891286
F1-ATPase epsilon subunit	1.1	0.0011		0.0026	AI171844
Mitochondrial fumarase	−1.1	0.0110		0.0181	J04473
Lipoprotein lipase	1.5	0.0484			L03294
24-kDa subunit of mitochondrial NADH dehydrogenase	1.4	0.0484			M22756
Bleomycin hydrolase	1.4	0.0158			D87336
Stress response					
Rapamycin and FKBP12 target-1 protein (rRAFT1)	1.1	0.0158	0.0358		U11681
Neuronal death protein	2.3	0.0484			D83697
Poly(ADP-ribose) polymerase	1.6	0.0077			U94340
Others					
Taipoxin-associated calcium binding protein-49 precursor	−1.2	0.0032	0.0119		U15734
Cytosolic resiniferatoxin binding protein RBP-26	−1.3	0.0289	0.0358		X67877
RNA binding protein (transformer-2-like)	−1.2	0.0110	0.0181		D49708
C15	−1.2	0.0002		0.0006	X82445
resection-induced TPI (rs11)	1.4	0.0011			AF007890
Anti-proliferative factor (BTG1)	−1.4	0.0484			L26268
Unknown					
EST	−1.5	0.0158	0.0474	0.0026	AA892280
EST	1.2	0.0484	0.0026		AI230632
EST	1.4	0.0484		0.0078	AA894234
EST	1.2	0.0484		0.0181	AF069782

[a]The fold change was calculated between mean values of control (n = 6) and LH-S rats (n = 6). Positive values indicate an increase, and negative a decrease in gene expression in the LH.
[b]Statistical comparison was made by Mann-Whitney test (two-tailed). Only significant *P*-values (< 0.05) are denoted.

Activation of serotonin 2 receptors reportedly diminished γ-amino butyric acid type A receptor current through PKC in prefrontal cortical neurons.[34] Expression changes in the *Htr2a* and PKCε genes in LH may indicate a functional link between the two systems in the depressive state. The precise role of neurexophilin 4 in the intercellular signaling system remains unclear,[35,36] but the gene may underlie a depression/stress-related physiological pathway that cannot be corrected using TCAs or SSRIs (Table 1).

Of the LH-associated genes identified from the FC, LIMK-1 (LIM domain kinase 1: *Limk1*) displayed the most dramatic decrease, a 9.5-fold reduction compared with control levels (Table 1). Transcriptional levels were not completely normalized by imipramine or fluoxetine treatment. This

Table 2 LH-associated transcripts in the hippocampus

Functional Groups	*Fold change*[a]	*P-value*[b]			*Accession No.*
		Cont vs *LH-S*	*LH-S* vs *LH-F*	*LH-S* vs *LH-I*	
Receptor					
HGL-SL1 olfactory receptor pseudogene	−2.0	0.0005	0.0358		AF091574
olfactory receptor-like protein (SCR D-9)	−1.4	0.0050			AF034899
heparin-binding fibroblast growth factor receptor 2	−2.4	0.0373			L19112
HFV-FD1 olfactory receptor	−2.5	0.0019			AF091575
Ion channel/Transporter					
Dri 27/ZnT4 protein (zinc transporter)	1.2	0.0464	0.0181		Y16774
Chloride channel RCL1	−1.1	0.0373	0.0181		D13985
High-Affinity L-proline transporter	−1.3	0.0050		0.0078	M88111
Plasma membrane CA2+-ATPase isoform 3	−1.4	0.0018			M96626
Signal transduction					
Paranodin	1.2	0.0213	0.0078		AF000114
Arl5 (ADP-ribosylation factor-like 5)	1.4	0.0213			AA956958
Grb14	−1.4	0.0213			AF076619
Neurotransmission					
Synuclein SYN1	−1.2	0.0213	0.0358		S73007
Alpha-soluble NSF attachment protein	−1.1	0.0213		0.0078	X89968
Rab13	−1.9	0.0005		0.0358	M83678
Rab3b	−1.6	0.0213			AA799389
GTP-binding protein (ral B)	−2.0	0.0110			L19699
Neural growth/ structure					
Tuba1 (Alpha-tubulin)	1.2	0.0213	0.0006		AA892548
Zinc-finger protein AT-BP2	−1.4	0.0213			X54250
CRP2 (cysteine-rich protein 2)	−1.4	0.0373			D17512
Nfyb CCAAT binding transcription factor of CBF-B/NFY-B	−1.4	0.0373			AA817843
Decorin	−2.2	0.0213			AI639233
Metabolic enzymes					
NADH-cytochrome b-5 reductase	−1.1	0.0110	0.0358	0.0181	AI229440
Siat5 (Sialyltransferase 5)	−1.7	0.0050	0.0078		X76988
24-kDa mitochondrial NADH dehydrogenase precursor	−1.4	0.0373			M22756
2-oxoglutarate carrier	−1.4	0.0110			U84727
Soluble cytochrome b5	−1.5	0.0110			AF007107
Stress response					
Ischemia responsive 94 kDa protein (irp94)	−1.4	0.0050			AF077354
MHC class I antigen	−1.5	0.0373			AF074609
Others					
RNA splicing-related protein	−1.4	0.0373			AI044739
Aes Amino-terminal enhancer of split	−1.4	0.0153			AA875427
Proteasome RN3 subunit	−1.5	0.0110			L17127
Unknown					
EST	1.5	0.0274	0.0358		AA799488
EST	1.4	0.0373	0.0078		AA858617
EST	1.2	0.0213	0.0026		AA892817
EST	1.2	0.0050	0.0026		AA892238
EST	1.1	0.0213	0.0026		AA799893
EST	1.1	0.0050	0.0006		AA799784
EST	−1.5	0.0213	0.0358		AA799525
EST	1.3	0.0373		0.0078	AA893039
EST	−1.1	0.0373		0.0358	AI007820
EST	−1.3	0.0373		0.0358	AA875348
EST	2.4	0.0213			AA875633
EST	1.9	0.0373			AI229655
EST	1.5	0.0373			AA955477
EST	1.5	0.0213			AA893569
EST	1.4	0.0464			AA800803
EST	−1.6	0.0274			AI639477
EST	−1.6	0.0110			AA892353

[a]The fold change was calculated between mean values of control ($n=6$) and LH-S rats ($n=6$). Positive values indicate an increase, and negative values (in red) a decrease in gene expression in the LH.
[b]Statistical comparsion was made by Mann-Whitney test (two-tailed). Only significant *P*-values (<0.05) are denoted.

Table 3 Gene expression levels evaluated by quantitative RT-PCR and comparisons with the results from microarray analysis

	Frontal cortex				*Hippocampus*			
	LIMK-1	*HTR2A*	*PGDS*	*IP3R*	*SNAP*	*SYN1*	*bFGFR2*	*Ca^{2+}-ATPase*
Control	1.00±0.42	1.00±0.57	1.00±0.19	1.00±0.48	1.00±0.36	1.00±0.44	1.00±0.21	1.00±0.31
LH-S	0.49±0.07	0.36±0.06	1.64±0.25[a]	0.97±0.20	0.61±0.14	0.54±0.17	0.88±0.23	0.80±0.37
LH-F	0.50±0.06	0.57±0.26	1.10±0.20	0.52±0.15	0.86±0.14	0.65±0.23	0.65±0.11	0.80±0.14
LH-I	0.44±0.08	0.53±0.08[b]	0.81±0.33	0.72±0.23	1.45±0.51	0.30±0.07	0.52±0.16	0.70±0.29
Fold change evaluated by RT-PCT (Cont *vs* LH-S)	−2.0	−2.8	1.6	−1.0	−1.6	−1.9	−1.1	−1.3
Fold change evaluated by microarray (Cont *vs* LH-S)	−9.5	−1.6	1.3	−1.1	−1.1	−1.2	−2.4	−1.4

The expression level of each gene is normalized to that of the GAPDH gene (mean±SE, $n=6$, each in control and LH-S, $n=5$, each in LH-F and LH-I). The gene abbreviations are: LIMK-1, LIM domain kinase 1; HTR2A, 5-hydroxytryptamine (serotonin) receptor 2A; PGDS, prostaglandin D synthetase; IP3R, inositol-1,4,5-triphosphate receptor type 1; SNAP, synaptosomal-associated protein; SYN1, synuclein 1; bFGFR2, heparin-binding fibroblast growth factor receptor 2; Ca^{2+}-ATPase, plasma membrane Ca^{2+}-ATPase isoform 3.
[a]$P<0.05$ (control *vs* LH-S).
[b]$P<0.05$ (LH-S *vs* LH-I) by Mann–Whitney test (two-tailed).

partial recovery might be due to the low level of normal transcription and the large variation of expression values (supplementary Table S3). We therefore performed real-time RT-PCR to confirm the expression profile of *Limk1*, and detected a two-fold decrease in LH compared to control animals. This reduction was not recovered by antidepressant treatments (Table 3). *Limk1* is expressed in both fetal and adult nervous systems, and shows ubiquitous expression in the brain with the strongest expression in adult cerebral cortex.[37] Recently, *Limk1*-knockout mice were reported to show abnormalities in spine morphology and enhanced long-term potentiation, accompanied by alterations in fear response and spatial learning.[38] A test of depression-related behavioral parameters in these mice would be intriguing. Additional reports that depressive patients frequently manifest subcortical hyperintensity near frontal white matter ('myelin pallor' on histological examination)[39] suggest that LIMK1 may be involved in an as yet undetermined intercellular signaling pathway disrupted in depression, as LIMK1 is known to phosphorylate myelin basic proteins.[40]

Our criteria for selecting 'altered' transcripts in LH compared to control animals may have been conservative and inadvertently excluded many potential candidates. Decreased levels of brain-derived neurotrophic factor (BDNF) recoverable by antidepressant treatment have been reported in patients with depression.[41,42] Although we could not detect any significant difference in expression between control and LH-S animals, we found that expression of BDNF in the FC was increased in LH-I animals compared with LH-S and control animals (supplementary Table S3).

LH-associated Transcripts Specific to the HPC and Common to Both the FC and HPC

In contrast to the FC, most LH-associated genes in the HPC showed decreased expressions on the induction of LH (Table 2). Genes coding for receptors were downregulated in both regions, although there was no overlap between the two groups of receptors. This category included three olfactory receptor-like genes, *HGL-SL1* olfactory pseudogene, olfactory receptor-like protein (*SCRD-9*) and *HFV-FD1* olfactory receptor. Although these are thought to encode G protein-coupled receptors with seven transmembrane domains, the biological functions are unclear. Heparin-binding fibroblast growth factor receptor 2 (*Fgfr2*) genes were also downregulated in LH-S, but were unaffected by antidepressants (Table 2). We also found a reduction in the *N*-methyl-D-aspartate receptor 2A (NMDAR 2A) subunit gene in three of six LH-S animals. Fgfr2 reduces NMDAR 2A subunit mRNA levels via a receptor-mediated mechanism.[43] Chronic administration of antidepressants decreases the expression of NMDA receptor subunit genes and radioligand binding to the receptor.[42] This discrepancy warrants further investigation, to determine the role of this growth factor and the NMDA receptor genes in depression. All the LH-associated genes defined as involved in neurotransmission were also downregulated in this study (Table 2). The hippocampus is well known as a region of the brain that is highly susceptible to stress.[44,45] Recent studies have demonstrated that repeated stress causes shortening and debranching of dendrites in the CA3 region of the HPC and suppresses neurogenesis of granule neurons in the dentate gyrus.[45,46] In addition, chronic antidepressant treatment increases cell populations and neurogenesis in the rat hippocampus.[15] The extensive suppression of gene expression observed in our LH model may be related to phenotypic changes in the hippocampus produced by stress.

An unexpected finding was the scarcity of common transcripts between the two areas of brain. Of the LH-associated genes, only those coding for the 24-kDa mitochondrial NADH dehydrogenase and Dri27/ZnT4 (zinc transporter) were common to both the FC and HPC (Tables 1 and 2). However, the direction of change differed between the two regions. This selectivity was also seen in genes that were not affected by LH, but displayed a response to

Table 4 List of genes contributing to the first component in principal component analysis

Brain region[a]	*Eigenvalue*	*Gene name*[b]	Function[c]	*Fold change*	*Accession no*	Locus[d]
Frontal cortex	0.2197	Rapamycin and FKBP12 target-1 protein (rRAFT)	Stress response	1.1	U11681	5q36
	0.2194	F1-ATPase epsilon subunit	Metabolic enzyme	1.1	AI171844	20q13.3
	0.1965	Jagged2 precursor	Neuronal growth / structure	1.3	U70050	14q32
	0.1929	24-kDa subunit of mitochondrial NADH dehydrog	Metabolic enzyme	1.4	M22756	18p11.31-p11.2
	0.1876	Bleomycin hydrolase	Metabolic enzyme	1.4	D87336	17q11.2
	0.1820	EST	Unknown	1.4	AA894234	—
	0.1760	Poly(ADP-ribose) polymerase	Stress response	1.6	U94340	1q41-q42
	0.1617	EST	Unknown	1.2	AI230632	—
	0.1531	Resection-induced TPI (rs11)	Others	1.4	AF007890	12p13
	0.1525	EST	Unknown	1.2	AF069782	—
Hippocampus	0.2114	HGL-SL1 olfactory receptor pseudogene	Receptor	−2.0	AF091574	—
	0.2092	Proteasome RN3 subunit	Others	−1.5	L17127	1q21
	0.2019	24-kDa mitochondrial NADH dehydrogenase prec	Metabolic enzyme	−1.4	M22756	18p11.31-p11.2*
	0.1997	HFV-FD1 olfactory receptor	Receptor	−2.5	AF091575	—
	0.1983	Soluble cytochrome b5	Metabolic enzyme	−1.5	AF007107	18q23*
	0.1865	2-Oxoglutarate carrier	Metabolic enzyme	−1.4	U84727	17p13.3
	0.1845	Grb14	Signal transduction	−1.4	AF076619	2q22-q24
	0.1626	EST	Unknown	−1.6	AA892353	—
	0.1606	GTP-binding protein (ral B)	Signal transduction	−2.0	L19699	2cen-q13
	0.1595	Rab3b	Signal transduction	−1.6	AA799389	1p32-p31*

[a]The 10 largest contributing genes to the first component in each region are listed.

[b]The genes in black indicate those up-regulated in LH animals compared to controls, while genes in red are down-regulated.

[c]The gene functions are color coded according to functional properties.

[d]*indicates that the chromosomal region shows genetic linkage to bipolar disorder.

treatment with fluoxetine, imipramine or both. In this case, from the three subsets (green, light blue and purple areas in Figure 4), five of 105 transcripts were common to both the FC and HPC (supplementary Tables S3 and S4). These findings may highlight region-specific molecular mechanisms involved in the etiology of LH. In human studies, decreased mitochondrial function was demonstrated in the basal ganglia of chronic schizophrenics,[47,48] and inhibition of mitochondrial respiratory complex I activity was reported as a cellular pathology of Parkinson's disease.[49,50] Evidence, including that of decreased ATP in frontal lobes detected in depressive patients,[51] has generated speculation about the role of mitochondrial dysfunction in depression.[52,53] NADH dehydrogenase is located on human chromosome 18 at p11.31–p11.2, a susceptibility region for affective disorder and schizophrenia.[3,54,55] These data suggest a possible link between mitochondrial NADH dehydrogenase and neuropsychiatric illnesses, including depression. The observed alteration in levels of a zinc transporter gene may tie in with recent reports that zinc exerts an antidepressant-like effect in the rodent forced swimming test,[56] and that patients with major depression demonstrate lower serum zinc levels.[57] This may imply perturbed zinc metabolism in depression, but the precise mechanisms are poorly understood.

Given that imipramine was more effective in improving LH behavior than fluoxetine, it may seem contradictory that a larger number of LH-associated transcripts showed a greater response to fluoxetine than to imipramine (Figure 4). Imipramine-responsive transcripts are likely to play a more pivotal role in behavioral recovery.

We also applied parametric statistical analysis (Student's *t*-test) to our array data. The total number of transcripts detected was slightly lower in both the FC and HPC compared to numbers detected by nonparametric tests (3 and 12 fewer in the FC and HPC, respectively). Between the two statistical methods, 10 genes in the FC (32%) and three genes in the HPC (8%) were different (supplementary Tables S7 and S8).

PCA on Altered Transcripts

PCA is a mathematical technique that exploits essential factors to define patterns in data, reducing the effective dimensionality of gene-expression space without significant loss of information.[58] This technique can be applied to both genes and experiments as a means of classification. When genes are variables, the analysis creates a set of principal gene components highlighting features of genes that best explain their experimental responses. We used the LH-associated transcripts from the FC and HPC separately as variables in PCA, to allow for better visualization of the region-specific data sets. Figures 5a and b indicate the eigenvalue distributions on the components in the FC and HPC samples, respectively. The sudden drop in eigenvalues with increasing component number suggests that it is possible to select a small number of components modeling the gene-expression differences among rat groups. We chose a three-component model for both the FC and HPC, which

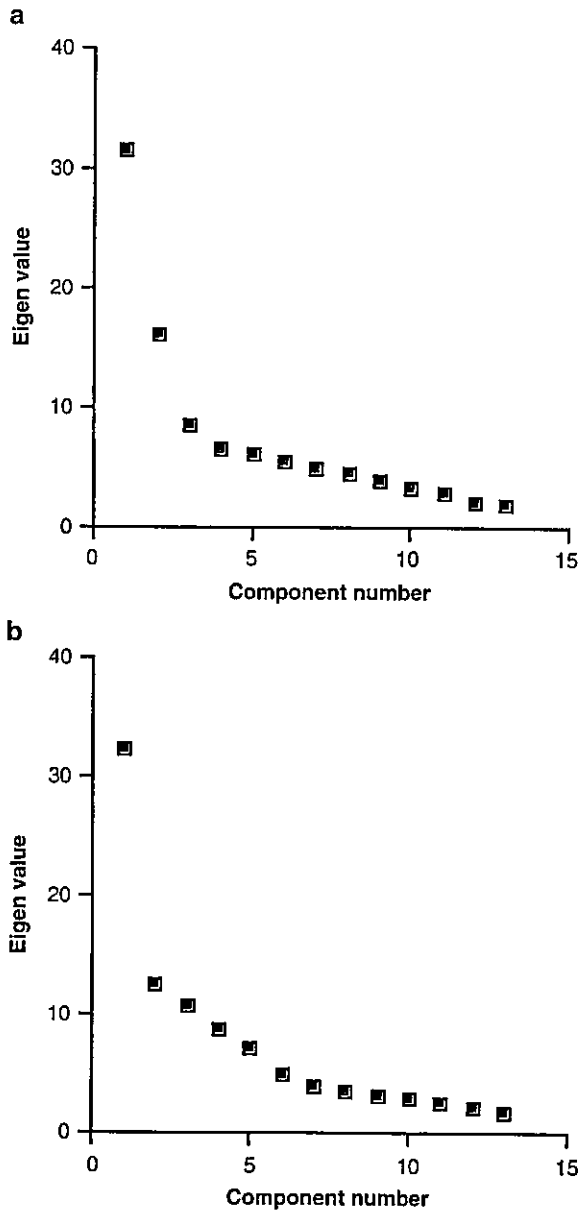

Figure 5 Component number *vs* eigenvalue in the FC (a) and the HPC (b).

explained 56% of the total variability seen in the 34 transcripts from the FC and the 48 transcripts from the HPC. The extracted dimensions represent the linear organization of data from independent systems. Each animal was plotted in a three-dimensional subspace (Figures 6a and b). The first components retain the maximal amount of correlated information (ie coordinated activity of genes) restricting the uncorrelated information to higher order components. In the FC, the first component (axis) showed good separation for the four experimental groups (control, LH-S, LH-F and LH-I), placing the antidepressant-treated groups between the control and LH-S groups. Table 4 shows

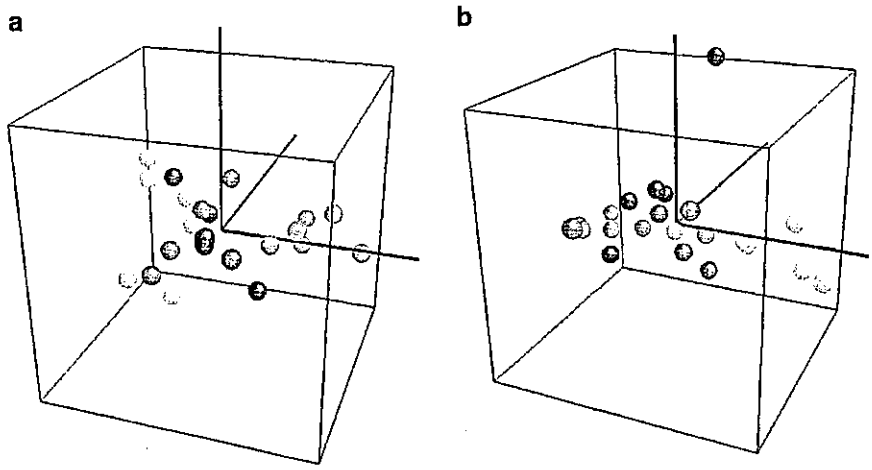

Figure 6 All animals were plotted with respect to the first (blue), second (green) and third (red) principal components. PCA was performed on transcripts listed in Table 1 (frontal cortex) (a) and Table 2 (hippocampus) (b). Yellow-colored dots represent control animals, green LH-S rats, red LH-F and blue LH-I.

transcripts from the FC that were arranged according to the magnitude of correlation with the first component (PC1) (those to the second and third components are shown in supplementary Table S5). They comprised genes for metabolic enzymes and stress responses. All genes listed in PC1 were increased in LH animals compared to controls. Among the genes coding for metabolic enzymes, the F1-ATPase epsilon subunit and 24-kDa subunit of mitochondrial NADH dehydrogenase are both localized to the mitochondria, further suggesting an important role for mitochondrial function in depression.[53] The second and third components in the FC did not further subdivide the experimental groups (supplementary figure S1). However, based on the data including the second component of PCA in the FC (supplementary Table S5), we speculate that genes responsible for neuronal growth and structure including *Limk1* could be key factors in depression/stress-related pathology. In downstream pathways, alterations of these genes may affect recruitment and maintenance of multiple neurotransmitter receptors.[38] In support of this theory, structural abnormalities have recently been reported in the frontal lobe white matter of depressive patients.[59]

According to PC1 in the HPC, LH-S rats were separated from controls, with the drug-treated animals being more closely localized than the LH-S group (Figure 6b). This highlights the limited efficacy of TCA and SSRI antidepressants against dysregulated genes in the HPC, although these drugs reversed the behavioral phenotype of LH rats. The genes contributing to PC1 from the HPC would therefore represent suitable targets for future novel antidepressants. PC1 in the HPC contained genes that were downregulated in LH rats and were clustered as metabolic enzyme and signal transduction (Table 4). The second component in the HPC detected eight genes that correlated with responsiveness to fluoxetine (supplementary Table S6 and Figure S2). One animal was separated from the others along the third component (Figure 6b). The reason for this was not clear. The animal may have suffered from highly aberrant expression of metabolic enzyme- and signal transduction-related genes and other transcripts (Table 4). Finally, the fact that the 24-kDa subunit of mitochondrial NADH dehydrogenase was extracted from both the FC and HPC with high eigenvalues is intriguing, suggesting that this gene may represent an indicator of depressive state. Moreover, the two genes, for soluble cytochrome b5 on 18q23 and Rab3 on 1p32-p31, mapped to reported linkage regions for bipolar disorder.[60]

MATERIALS AND METHODS

Animals and Experimental Design

Male Sprague–Dawley rats, 5–6-week old, weighing 150–180 g, were purchased from SLC (Shizuoka, Japan). They were housed three per cage under standard laboratory conditions, with access to food and water *ad libitum*. After 1 week of handling, the animals were used for experiments. Antidepressants, imipramine and fluoxetine were purchased from SIGMA (St Louis, MO, USA).

On day 1, animals were subjected to IS pretreatment (0.5 mA, 10 s duration, shock interval 1–5 s, 160 trials) in a Plexiglas chamber ($460\,W \times 200\,D \times 180\,H\,mm^3$, Muromachi, Tokyo, Japan). Two rats were processed simultaneously using two chambers. Control rats were placed for 1 h in the same chambers, but no shocks were administered.

On day 2, to evaluate escape and avoidance performance, avoidance training was initiated 24 h after IS pretreatment in the same chamber, which had been converted to a two-way shuttle box by dividing it into two equal-sized compartments using an aluminum partition. The partition included a square gate ($6 \times 6\,cm^2$), through which animals

could move into the adjacent compartment. Animals were subjected to 15 avoidance trials with 30 s intervals. In each trial, 0.5 mA of current was applied via the grid floor during the first 3 s. If an animal crossed the gate and moved to the other compartment within this period (escape response), the shock was terminated. Failures in escape response were counted as a measure of LH. Animals were defined as suffering from LH when they showed eight or more failures during a session. Control rats and a proportion of LH rats (LH-S) were administered saline once a day for three consecutive days, starting on day 2 after the avoidance trial. The remaining LH animals were treated using either imipramine (25 mg/kg, i.p.) (LH-I) or fluoxetine (5 mg/kg, i.p.) (LH-F).

On day 5, 30 min after the final injection, rats were tested for escape ability under escapable shock conditions. Among LH-I and LH-F rats, only those animals that showed a >50% successful escape response (ie <8 failures in the 15 trials; all LH-I rats fulfilled this criterion) were used for gene-expression analysis.

The present protocol was approved by the RIKEN animal committee.

RNA Preparation and Array Hybridization

Animals were killed on day 6, 24 h after the final electroshock procedure. Total RNA was extracted from the FC (defined as the region anterior to the genu of corpus callosum, with the ventral olfactory structures depleted) and HPC using an acid guanidium thiocyanate/phenol chloroform extraction method (ISOGEN, NIPPON Gene, Toyama, Japan). Double-stranded cDNA was synthesized from 10 μg of total RNA using the SuperScript Choice System (Invitrogen, Carlsbad, CA, USA) and a primer containing poly (dT) and a T7 RNA polymerase promoter sequences (Geneset, La Jolla, CA, USA). Biotin-labeled cRNA was synthesized from cDNA using an Enzo BioArray High Yield RNA Transcript Labeling kit (Enzo Diagnostics, Santa Clara, CA, USA). After fragmentation, 15 μg of cRNA was hybridized for 16 h at 45°C to a U34A chip (Affymetrix, Santa Clara, CA, USA) that contained probes for over 8000 transcripts, including all known rat genes (http://www.affymetrix.com/products/netaffx.html). After hybridization, arrays were washed automatically and stained with streptavidin–phycoerythrin using the fluidics system. Chips were scanned using a GeneArray scanner (Affymetrix).

Data Analysis

All samples were scaled to a target intensity of 100. Data analysis was performed using Microarray Suite 4.0 (Affymetrix) and GeneSpring 4.1 (Silicon Genetics, Redwood, CA, USA). Transcripts with an 'average difference' (as described in the GeneChip software) of <20 for each probe set in controls were excluded (5157 genes were selected out of 8799). From the remaining transcripts, those that gave an 'absolute call' of 'P' (present) for at least four samples in six for control and LH-S rats were considered for further analysis (3541 genes were chosen).

Before statistical analysis, each transcript was converted into a logarithmic value and normalized to itself by making a synthetic positive control and dividing all measurements by this control, assuming that the control value was at least 0.01. A synthetic control is the median of the transcript's expression values over all the samples. Two-group comparison was conducted for each transcript by a Mann–Whitney test between: (i) control and LH-S groups, (ii) LH-S and LH-F groups and (iii) LH-S and LH-I groups. The results are illustrated as a Venn diagram (Figure 2), where the overlapping areas representing (i)-, (ii)- and (iii)-type comparisons include transcripts that were selected solely using Mann–Whitney test ($P<0.05$) and Student's t-test ($P<0.05$). Transcripts in non-overlapping areas represent genes whose expressional changes between the two states displayed ⩾1.4-fold difference, in addition to fulfilling the P-value criteria. We also evaluated these selected transcripts by implementing the Benjamin and Hochbery False Discovery Rate program included in the GeneSpring software package. The differential gene expressions revealed by the microarray chips were examined using real-time quantitative reverse transcription (RT)-PCR, with a LightCycler and RNA Amplification kit SYBR Green I (Roche, Basel, Swizerland).

Principal Component Analysis

PCA is a statistical method for determining the coordinate transformation that explains the maximum amount of variance for the data.[25] PCA finds the principal components and each component is mutually orthogonal. To calculate the transformation, data were first normalized with reference to each gene, and then sample mean and sample variance–covariance matrix S were calculated from estimates of the mean and variance–covariance matrix. From this symmetrical matrix S, an orthogonal basis was calculated by determining eigenvalues and eigenvectors according to the equation:

$$|S - \lambda_i E| = 0 \quad (1)$$

where E is an identity matrix and λ_i is the ith eigenvalue. i takes the value (1 to n), and n is the total number of genes.

$$SA_i = \lambda_i A_i \quad (2)$$

where A_i is the ith eigenvector (n-dimension). The first and ith principal components were calculated as follows: $PC1 = \sum A_1 D$, $PCi = \sum A_i D$, where A_1 is the eigenvector with maximum eigenvalue, and D is the n-dimensional data vector. The proportion of the ith component was the ith eigenvalue divided by the total sum of all eigenvalues. Animals were projected into the first three-dimensional component space.[62,63]

CONCLUSION

In an effort to better understand the molecular and genetic bases underlying the pathophysiology of depressive disorder and to improve the rationale for the design of antidepressant drugs, we have performed DNA microarray analysis using an animal model of depression. Using Affymetrix GeneChip arrays, we have screened over 8000 rat genes and

ESTs, and identified 82 distinct transcripts (Tables 1 and 2, and supplementary Tables S1 and S2) in the FC and HPC that are relevant to LH and responsive to conventional antidepressants. To date, the strategy for designing antidepressive drugs is based on the serendipitous paradigm that the augmentation of monoaminergic activity in the central nervous system leads to therapeutic benefits.[1] However, currently available drugs have several drawbacks in terms of slow onset of action and intractable disease presents in approximately one-third of all depressive patients.[61] Given the genetically complex nature of human depression, we recognize that the present study can explain only limited aspects of depression pathology. Nevertheless, we believe that this study could give rise to new ideas for probing into the genetic mechanisms of human affective disorder and for refining the development of advanced therapeutics.

DUALITY OF INTEREST

None declared

ACKNOWLEDGEMENTS

We would like to thank Shuichi Tsutsumi and Hiroko Meguro for assistance with microarray data analysis, Yuichi Ishitsuka, Yuki Iijima and Shin-ichi Ohno for help with animal experiments, Kazuo Yamada for useful comments and Joanne Meerabux for critical reading of this manuscript. This study was partly supported by Grants-in-Aid for Young Scientists (B) (No. 13770566) from the Ministry of Education, Culture, Sports and Technology (MEXT).

ABBREVIATIONS

BDNF	*brain-derived neurotrophic factor*
EST	*expressed sequence tag*
FC	*frontal cortex*
HPC	*hippocampus*
IS	*inescapable shocks*
LH	*learned helplessness*
LH-F	*LH rats treated with fluoxetine*
LH-I	*LH rats treated with imipramine*
LH-S	*LH rats treated with saline*
NMDA	*N-methyl-D-aspartate*
NREM	*nonrapid eye movement*
PKC	*protein kinase C*
RT	*reverse transcription*
SSRI	*selective serotonin reuptake inhibitor*
TCA	*tricyclic antidepressant*

SUPPLEMENTARY INFORMATION

Supplementary Information accompanies the paper on the TPJ website (http://www.nature.com/tpj).

REFERENCES

1 Nestler EJ, Barrot M, DiLeone RJ, Eisch AJ, Gold SJ, Monteggia LM. Neurobiology of depression. *Neuron* 2002; 34: 13–25.
2 Fava M, Kendler KS. Major depressive disorder. *Neuron* 2000; 28: 335–341.
3 Detera-Wadleigh SD, Badner JA, Berrettini WH, Yoshikawa T, Goldin LR, Turner G *et al*. A high-density genome scan detects evidence for a bipolar-disorder susceptibility locus on 13q32 and other potential loci on 1q32 and 18p11.2. *Proc Natl Acad Sci USA* 1999; 96: 5604–5609.
4 Overmier JB, Seligman ME. Effects of inescapable shock upon subsequent escape and avoidance responding. *J Comp Physiol Psychol* 1967; 63: 28–33.
5 Telner JI, Singhal RL. Psychiatric progress. The learned helplessness model of depression. *J Psychiatr Res* 1984; 18: 207–215.
6 Geoffroy M, Scheel-Kruger J, Christensen AV. Effect of imipramine in the 'learned helplessness' model of depression in rats is not mimicked by combinations of specific reuptake inhibitors and scopolamine. *Psychopharmacology* 1990; 101: 371–375.
7 Nankai M, Yamada S, Muneoka K, Toru M. Increased 5-HT2 receptor-mediated behavior 11 days after shock in learned helplessness rats. *Eur J Pharmacol* 1995; 281: 123–130.
8 Willner P. A Psychobiological Synthesis. In: *Depression*. John Wiley & Sons: New York 1985.
9 Ferguson SM, Brodkin JD, Lloyd GK, Menzaghi F. Antidepressant-like effects of the subtype-selective nicotinic acetylcholine receptor agonist, SIB-1508Y, in the learned helplessness rat model of depression. *Psychopharmacology* 2000; 152: 295–303.
10 Sherman AD, Petty F. Learned helplessness decreases [^{3}H]imipramine binding in rat cortex. *J Affect Disord* 1984; 6: 25–32.
11 Mac Sweeney CP, Lesourd M, Gandon JM. Antidepressant-like effects of alnespirone (S 20499) in the learned helplessness test in rats. *Eur J Pharmacol* 1998; 345: 133–137.
12 Musty RE, Jordan MP, Lenox RH. Criterion for learned helplessness in the rat: a redefinition. *Pharmacol Biochem Behav* 1990; 36: 739–744.
13 Drevets WC, Price JL, Simpson Jr JR, Todd RD, Reich T, Vannier M *et al*. Subgenual prefrontal cortex abnormalities in mood disorders. *Nature* 1997; 386: 824–827.
14 Jacobs BL, Praag H, Gage FH. Adult brain neurogenesis and psychiatry: a novel theory of depression. *Mol Psychiatry* 2000; 5: 262–269.
15 Malberg JE, Eisch AJ, Nestler EJ, Duman RS. Chronic antidepressant treatment increases neurogenesis in adult rat hippocampus. *J Neurosci* 2000; 20: 9104–9110.
16 Eriksson PS, Perfilieva E, Bjork-Eriksson T, Alborn AM, Nordborg C, Peterson DA *et al*. Neurogenesis in the adult human hippocampus. *Nat Med* 1998; 4: 1313–1317.
17 Martin P, Soubrie P, Simon P. The effect of monoamine oxidase inhibitors compared with classical tricyclic antidepressants on learned helplessness paradigm. *Progr Neuro-Psychopharmacol Biol Psychiatry* 1987; 11: 1–7.
18 Nakagawa Y, Ishima T, Ishibashi Y, Tsuji M, Takashima T. Involvement of GABAB receptor systems in action of antidepressants. II: Baclofen attenuates the effect of desipramine whereas muscimol has no effect in learned helplessness paradigm in rats. *Brain Res* 1996; 728: 225–230.
19 Nakagawa Y, Sasaki A, Takashima T. The GABA(B) receptor antagonist CGP36742 improves learned helplessness in rats. *Eur J Pharmacol* 1999; 381: 1–7.
20 Tejedor-Real P, Mico JA, Maldonado R, Roques BP, Gibert-Rahola J. Implication of endogenous opioid system in the learned helplessness model of depression. *Pharmacol Biochem Behav* 1995; 52: 145–152.
21 Anthony JP, Sexton TJ, Neumaier JF. Antidepressant-induced regulation of 5-HT(1b) mRNA in rat dorsal raphe nucleus reverses rapidly after drug discontinuation. *J Neurosci Res* 2000; 61: 82–87.
22 Bristow LJ, O'Connor D, Watts R, Duxon MS, Hutson PH. Evidence for accelerated desensitisation of 5-HT_{2C} receptors following combined treatment with fluoxetine and the 5-HT_{1A} receptor antagonist, WAY 100,635, in the rat. *Neuropharmacology* 2000; 39: 1222–1236.
23 Tordera RM, Monge A, Del Rio J, Lasheras B. Antidepressant-like activity of VN2222, a serotonin reuptake inhibitor with high affinity at 5-HT1A receptors. *Eur J Pharmacol* 2002; 442: 63–71.
24 Mimics K, Middleton AF, Lewis AD, Levitt P. Analysis of complex brain disorders with gene expression microarrays: schizophrenia as a disease of the synapse. *Trends Neurosci* 2001; 24: 479–486.
25 Raychaudhuri S, Stuart JM, Altman RB. Principal components analysis to summarize microarray experiments: application to sporulation time series. *Pacific Symp Biocomput* 2000: 455–466.
26 Wurmbach E, Yuen T, Ebersole BJ, Sealfon SC. Gonadotropin-releasing hormone receptor-coupled gene network. *J Biol Chem* 2001; 276: 47195–47201.
27 Papolos DF, Yu YM, Rosenbaum E, Lachman HM. Modulation of learned helplessness by 5-hydroxytryptamine2A receptor antisense oligodeoxynucleotides. *Psychiatr Res* 1996; 63: 197–203.
28 Wu J, Kramer GL, Kram M, Steciuk M, Crawford IL, Petty F. Serotonin and learned helplessness: a regional study of 5-HT1A, 5-HT2A receptors

and the serotonin transport site in rat brain. *J Psychiatr Res* 1999; 33: 17–22.
29 Pandey GN, Pandey SC, Dwivedi Y, Sharma RP, Janicak PG, Davis JM. Platelet serotonin-2A receptors: a potential biological marker for suicidal behavior. *Am J Psychiatry* 1995; 152: 850–855.
30 Velbinger K, De Vry J, Jentzsch K, Eckert A, Henn F, Muller WE. Acute stress induced modifications of calcium signaling in learned helpless rats. *Pharmacopsychiatry* 2000; 33: 132–137.
31 Aldenhoff JB, Dumais-Huber C, Fritzsche M, Sulger J, Vollmayr B. Altered Ca(2+)-homeostasis in single T-lymphocytes of depressed patients. *J Psychiatr Res* 1997; 31: 315–322.
32 Hayaishi O. Molecular mechanisms of sleep–wake regulation: a role of prostaglandin D2. *Philos Trans R Soc London—Ser B Biol Sci* 2000; 355: 275–280.
33 Mizoguchi A, Eguchi N, Kimura K, Kiyohara Y, Qu WM, Huang ZL *et al.* Dominant localization of prostaglandin D receptors on arachnoid trabecular cells in mouse basal forebrain and their involvement in the regulation of non-rapid eye movement sleep. *Proc Natl Acad Sci USA* 2001; 98: 11674–11679.
34 Feng J, Cai X, Zhao J, Yan Z. Serotonin receptors modulate GABA(A) receptor channels through activation of anchored protein kinase C in prefrontal cortical neurons. *J Neurosci* 2001; 21: 6502–6511.
35 Missler M, Hammer RE, Sudhof TC. Neurexophilin binding to alpha-neurexins. A single LNS domain functions as an independently folding ligand-binding unit. *J Biol Chem* 1998; 273: 34716–34723.
36 Missler M, Sudhof TC. Neurexophilins form a conserved family of neuropeptide-like glycoproteins. *J Neurosci* 1998; 18: 3630–3638.
37 Nunoue K, Ohashi K, Okano I, Mizuno K. LIMK-1 and LIMK-2, two members of a LIM motif-containing protein kinase family. *Oncogene* 1995; 11: 701–710.
38 Sarmiere PD, Bamburg JR, Meng Y, Zhang Y, Tregoubov V, Janus C *et al.* Head, neck, and spines. A role for LIMK-1 in the hippocampus. Abnormal spine morphology and enhanced LTP in LIMK-1 knockout mice. *Neuron* 2002; 35: 3–5.
39 Steffens DC, Krishnan KR. Structural neuroimaging and mood disorders: recent findings, implications for classification, and future directions. *Biol Psychiatry* 1998; 43: 705–712.
40 Okano I, Hiraoka J, Otera H, Nunoue K, Ohashi K, Iwashita S *et al.* Identification and characterization of a novel family of serine/threonine kinases containing two N-terminal LIM motifs. *J Biol Chem* 1995; 270: 31321–31330.
41 Altar CA. Neurotrophins and depression. *Trends Pharmacol Sci* 1999; 20: 59–61.
42 Skolnick P. Antidepressants for the new millennium. *Eur J Pharmacol* 1999; 375: 31–40.
43 Brandoli C, Sanna A, De Bernardi MA, Follesa P, Brooker G, Mocchetti I. Brain-derived neurotrophic factor and basic fibroblast growth factor downregulate NMDA receptor function in cerebellar granule cells. *J Neurosci* 1998; 18: 7953–7961.
44 Gould E, Tanapat P. Stress and hippocampal neurogenesis. *Biol Psychiatry* 1999; 46: 1472–1479.
45 McEwen BS. Stress and hippocampal plasticity. *Annu Rev Neurosci* 1999; 22: 105–122.
46 McEwen BS. Effects of adverse experiences for brain structure and function. *Biol Psychiatry* 2000; 48: 721–731.
47 Prince JA, Blennow K, Gottfries CG, Karlsson I, Oreland L. Mitochondrial function is differentially altered in the basal ganglia of chronic schizophrenics. *Neuropsychopharmacology* 1999; 21: 372–379.
48 Maurer I, Zierz S, Moller H. Evidence for a mitochondrial oxidative phosphorylation defect in brains from patients with schizophrenia. *Schizophr Res* 2001; 48: 125–136.
49 Jha N, Jurma O, Lalli G, Liu Y, Pettus EH, Greenamyre JT *et al.* Glutathione depletion in PC12 results in selective inhibition of mitochondrial complex I activity. Implications for Parkinson's disease. *J Biol Chem* 2000; 275: 26096–26101.
50 Chinopoulos C, Adam-Vizi V. Mitochondria deficient in complex I activity are depolarized by hydrogen peroxide in nerve terminals: relevance to Parkinson's disease. *J Neurochem* 2001; 76: 302–306.
51 Volz HP, Rzanny R, Riehemann S, May S, Hegewald H, Preussler B *et al.* 31P magnetic resonance spectroscopy in the frontal lobe of major depressed patients. *Eur Arch Psychiatr Clin Neurosci* 1998; 248: 289–295.
52 Jaksch M, Lochmuller H, Schmitt F, Volpel B, Obermaier-Kusser B, Horvath R. A mutation in mt tRNALeu(UUR) causing a neuropsychiatric syndrome with depression and cataract. *Neurology* 2001; 57: 1930–1931.
53 Kato T. The other, forgotten genome: mitochondrial DNA and mental disorders. *Mol Psychiatry* 2001; 6: 625–633.
54 Yoshikawa T, Kikuchi M, Saito K, Watanabe A, Yamada K, Shibuya H *et al.* Evidence for association of the myo-inositol monophosphatase 2 (IMPA2) gene with schizophrenia in Japanese samples. *Mol Psychiatry* 2001; 6: 202–210.
55 Schwab SG, Hallmayer J, Lerer B, Albus M, Borrmann M, Honig S *et al.* Support for a chromosome 18p locus conferring susceptibility to functional psychoses in families with schizophrenia, by association and linkage analysis. *Am J Hum Genet* 1998; 63: 1139–1152.
56 Kroczka B, Branski P, Palucha A, Pilc A, Nowak G. Antidepressant-like properties of zinc in rodent forced swim test. *Brain Res Bull* 2001; 55: 297–300.
57 Maes M, Vandoolaeghe E, Neels H, Demedts P, Wauters A, Meltzer HY *et al.* Lower serum zinc in major depression is a sensitive marker of treatment resistance and of the immune/inflammatory response in that illness. *Biol Psychiatry* 1997; 42: 349–358.
58 Quackenbush J. Computational analysis of microarray data. *Nat Rev Genet* 2001; 2: 418–427.
59 Steingard RJ, Renshaw PF, Hennen J, Lenox M, Cintron CB, Yuoung AD *et al.* Smaller frontal lobe white matter volumes in depressed adolescents. *Biol Psychiatry* 2002; 52: 413–417.
60 Cowan WM, Kopnisky KL, Hyman SE. The human genome project and its impact on psychiatry. *Annu Rev Neurosci* 2002; 25: 1–50.
61 Skolnick P, Legutko B, Li X, Bymaster FP. Current perspectives on the development of non-biogenic amine-based antidepressants. *Pharmacol Res* 2001; 43: 411–423.
62 Crescenzi M, Giuliani A. The main biological determinants of tumor line taxonomy elucidated by a principal component analysis of microarray data. *FEBS Lett* 2001; 507: 114–118.
63 Landgrebe J, Welzl G, Metz T, van Gaalen MM, Ropers H, Wurst W *et al.* Molecular characterization of antidepressant effects in the mouse brain using gene expression profiling. *J Psychiatr Res* 2002; 36: 119–129.

Journal of Cerebral Blood Flow & Metabolism
24:212–223 © 2004 The International Society for Cerebral Blood Flow and Metabolism
Published by Lippincott Williams & Wilkins, Inc., Baltimore

Genome-wide Gene Expression Analysis for Induced Ischemic Tolerance and Delayed Neuronal Death Following Transient Global Ischemia in Rats

*§Nobutaka Kawahara, *Yan Wang, *†Akitake Mukasa, *§Kazuhide Furuya, ‖Tatsuya Shimizu, ‡Takao Hamakubo, †Hiroyuki Aburatani, ‡Tatsuhiko Kodama, and *§Takaaki Kirino

**Department of Neurosurgery, Faculty of Medicine, University of Tokyo, Japan; †Genomescience and ‡Molecular Biology Divisions, Research Center for Advanced Science and Technology, University of Tokyo, Japan; §SORST (Solution-Oriented Research for Science and Technology), Japan Science and Technology Cooperation (JST), Saitama, Japan; and ‖Department of Neurosurgery, Gunma University School of Medicine, Japan.*

Summary: Genome-wide gene expression analysis of the hippocampal CA1 region was conducted in a rat global ischemia model for delayed neuronal death and induced ischemic tolerance using an oligonucleotide-based DNA microarray containing 8,799 probes. The results showed that expression levels of 246 transcripts were increased and 213 were decreased following ischemia, corresponding to 5.1% of the represented probe sets. These changes were divided into seven expression clusters using hierarchical cluster analysis, each with distinct conditions and time-specific patterns. Ischemic tolerance was associated with transient up-regulation of transcription factors (c-Fos, JunB Egr-1, -2, -4, NGFI-B), Hsp70 and MAP kinase cascade-related genes (MKP-1), which are implicated cell survival. Delayed neuronal death exhibited complex long-lasting changes of expression, such as up-regulation of proapoptotic genes (GADD153, Smad2, Dral, Caspase-2 and -3) and down-regulation of genes implicated in survival signaling (MKK2, and PI4 kinase, DAG/PKC signaling pathways), suggesting an imbalance between death and survival signals. Our study provides a differential gene expression profile between delayed neuronal death and induced ischemic tolerance in a genome-wide analysis, and contributes to further understanding of the complex molecular pathophysiology in cerebral ischemia.
Key Words: global ischemia—hippocampus—delayed neuronal death—ischemic tolerance—DNA microarray—gene expression.

Transient cerebral ischemia causes selective and delayed neuronal death in the vulnerable hippocampal CA1 region (Kirino 1982; Pulsinelli et al., 1982). Since this type of neuronal death occurs over several days, suggesting a potentially wide therapeutic window, its pathophysiological mechanisms have been intensively investigated as a model of ischemic neuronal injury. Various studies have provided evidence that cerebral ischemia induces transcriptional activation of a variety of genes (MacManus and Linnik 1997), particularly those related to stress response, cell death or survival (Chen et al., 1996; Chen et al., 1997; Chen et al., 1998; Nowak 1990), suggesting a close relationship with neuronal ischemic vulnerability. Based on these observations, various attempts have been made to identify differentially expressed mRNA by using subtractive hybridization (Wang et al., 2001) and PCR based techniques (Schwarz et al., 2002), which were expected to elucidate the complex molecular events leading to ischemic neuronal death. Despite these efforts, the underlying pathophysiological mechanisms remain unknown.

Recent advances in DNA microarray technology have provided tools to analyze the expression of thousands of genes in a single hybridization experiment (Lockhart and Winzeler 2000). In cerebral ischemia, this approach has been used to uncover key molecular events using a focal ischemia model (Keyvani et al., 2002; Kim et al., 2002; Raghavendra Rao et al., 2002; Soriano et al., 2000), and global ischemia or hypoxic models (Bernaudin et al., 2002; Jin et al., 2001). These studies, however, have limitations in evaluating global and sequential changes in gene expression related to cell death or survival, due to restricted time points, limited and biased transcripts represented on the array, and the nature of the sample analyzed.

Received June 12, 2003; accepted October 20, 2003.
This study was supported in part by a Grant-in-Aid from the Ministry of Education, Culture, Sports, Science and Technology, Japan, and by the Mitsubishi Foundation.
Address correspondence and reprint requests to N. Kawahara, Department of Neurosurgery, Faculty of Medicine, University of Tokyo, 7–3-1, Hongo, Bunkyo-ku, Tokyo, 113–8655, Japan; e-mail:kawahara-tky@umin.ac.jp

DOI: 10.1097/01.WCB.0000106012.33322.A2

Our study was designed to demonstrate global and sequential changes of gene expression during the process of ischemic neuronal death in the hippocampus. For this, we specifically analyzed a microdissected hippocampal CA1 region one to 48 hours after ischemia using an oligonucleotide-based DNA microarray containing approximately 7,000 full-length known or annotated genes and 1,000 EST clusters. We compared these changes with those during the induction of ischemic tolerance. It is widely known that hippocampal neurons can acquire resistance to ischemia when subjected to sublethal ischemia several days prior to lethal ischemia (for review, refer to Kirino, 2002). Comparison of global expression profiles during the process of ischemic cell death and ischemic tolerance, should lead to a better understanding of the molecular pathophysiology of ischemia.

MATERIALS AND METHODS

Animals

The experiments were performed on male Wistar SPF rats (280–320 g, Charles River, Yokohama, Japan). All animal-related procedures were conducted in accordance with guidelines for the care and use of laboratory animals set out by the National Institutes of Health.

Experimental Groups

Four groups of animals were used. In the first experiment (single ischemia experiment), histological assessment of global cerebral ischemia in the hippocampal CA1 sector was performed in rats subjected to sham operation (n = 6), two-minute (n = 8) or six-minute (n = 10) ischemia. In the second experiment (double ischemia experiment), induction of ischemic tolerance by two-minute ischemia was evaluated. In this group, rats were preconditioned by either sham operation with vertebral artery coagulation (n = 10) or two-minute ischemia (n = 10), and then subjected to six-minute ischemia three days later. The hippocampus was then examined as in the previous experiment. In the third experiment, samples of hippocampal CA1 sector of the animals subjected to sham operation (n = 15), two-minute (n = 30) or six-minute ischemia (n = 30) were analyzed for global mRNA expression (GeneChip experiment). In the final group, rats were subjected to sham, two-minute, or six-minute ischemia, and then sacrificed for *in situ* hybridization study.

Global Cerebral Ischemia

Global cerebral ischemia was induced by a modification of the four-vessel occlusion method (Pulsinelli et al., 1982). Rats were fixed in a stereotaxic frame under 1% halothane anesthesia. Both vertebral arteries were exposed under a microscope by drilling through the foramina, then coagulated and completely cut using fine-tipped bipolar forceps. Twelve hours later, under fasting conditions, the animals were intubated and put on a rodent respirator (Model 7025, Ugo Basile, Comerio, Italy) under 1.0% halothane anesthesia in a 30% O_2/ 70% N_2O mixture. The left femoral artery and vein were cannulated for blood pressure (BP) monitoring (Carrier Amplifier AP-601G, Nihon Kohden, Tokyo, Japan) and intravenous drug administration. The right femoral artery was also cannulated for exsanguination. Atropine sulfate (0.25mg/kg, ip) and amikacin (10mg/kg, ip) were administered. Rectal temperature was maintained at 37.5°C using a heating blanket (Animal Blanket Controller, Model ATB-1100, Nihon Kohden) for 30 minutes postischemia. Temporal muscle temperature was monitored with a thermometer (Model BAT-12, Physitemp Instruments, Clifton, NJ, USA) via a needle microprobe (MT-26/2, Physitemp Instruments) and kept at 37°C with a heating lamp. Cerebral ischemia was induced for either 2 or 6 minutes by occluding the bilateral common carotid arteries with clips. During ischemia, BP was lowered to 60 mmHg by exsanguination into a heparinized syringe from the right femoral artery, and electrical silence was confirmed by electroencepalogram (EEG) with needle electrodes connected to an amplifier (Bioelectric Amplifier AB-621G, Nihon Kohden, Tokyo, Japan). Following reperfusion, all physiological parameters were controlled for 30 minutes, and the animals were returned to their cages after extubation. Arterial blood samples were analyzed before, five, and 30 minutes after ischemia using a blood gas analyzer (Model 248, Chiron Diagnostics Ltd., Essex, UK) and a glucose analyzer (Glu-1, TOA Electronics Ltd., Tokyo, Japan). During the procedure, PaO_2 was maintained at 120–140 mmHg by adjusting inhaled O_2 concentration, and $PaCO_2$ at 35–40 mmHg by changing the respiratory rate. Base excess was corrected by intravenous injection of sodium bicarbonate and kept at −2.0 to 2.0 mEq/L. Sham operated animals were similarly treated except for vertebral artery coagulation and carotid artery clipping. In the double ischemia group (tolerance experiment), vertebral artery coagulation was performed in the sham operation.

Histological Assessment of Ischemic Neuronal Injury

Seven days after ischemia or sham operation, the animals were put under 2% halothane anesthesia and then fixed by transcardiac perfusion with 4% paraformaldehyde in 0.1mol/L phosphate buffer (pH = 7.4). The brains were left *in situ* for three hours, removed, and post-fixed overnight at 4°C, then embedded in paraffin. Coronal sections (4-μm thickness) obtained from the dorsal hippocampus (approximately 3.8 mm from bregma) (Paxinos and Watson 1986) were stained with hematoxylin and eosin, and the number of intact neurons was counted in a blind fashion along the pyramidal layer of the CA1 sector for 1 mm. The neuronal densities obtained (cells/mm) were averaged for each hemisphere and compared. In the first single ischemia group, one-way analysis of variance (ANOVA) with significance set at $p<0.05$ was used. In the second group (double ischemia), two-tailed unpaired Student's t-test with significance set at $p<0.05$ was used. All the data was shown as mean ±SD.

Microarray Experiment

Rats were subjected to sham operation, two-minute or six-minute ischemia, then sacrificed by decapitation under deep pentobarbital anesthesia at 1, 3, 12, 24, and 48 hours. The brains were quickly removed, frozen in 2-methylbutane at −20°C, and stored at −80°C. The brains were cut into 2-mm coronal sections and the dorsal hippocampal CA1 sector was dissected, under a microscope, at −20°C. Total RNA was extracted from pooled samples obtained from three rats using Isogen reagent (NipponGene Inc, Toyama, Japan), following the manufacturer's protocols. The quality of total RNA was verified by gel electrophoresis and $OD_{260/280nm}$ ratios.

Five micrograms of total RNA from each sample was used to synthesize biotin-labeled cRNA, which was then hybridized to a high-density oligonucleotide array (GeneChip Rat RG-U34A

array; Affymetrix Inc., Santa Clara, CA, USA), following a previously published protocol with minor modifications (Ishii et al., 2000). This array contains 8,799 probe sets derived from full-length or annotated genes (7,000 genes) as well as 1,000 EST clusters, which were selected from the Unigene Build 34, Genbank 110, and the dbEST databases. After washing, arrays were stained with streptavidin-phycoerythrin (Molecular Probes, Inc., Eugene, OR, USA) and analyzed by a Hewlett-Packard Scanner to collect primary data. The GeneChip 3.3 software (Affymetrix) was used to calculate the average difference for each gene probe on the array, which was shown as an intensity value of gene expression, defined by Affymetrix, using the proprietary algorithm. The average difference has been shown to quantitatively reflect the abundance of a particular mRNA molecule in a population (Ishii et al., 2000; Lockhart et al., 1996). To allow comparisons between multiple arrays, the average differences were normalized for each array by assigning the average of overall average difference values to be 100. A value of 20 was assigned to all average differences below 20.

Duplicate measurements were conducted for the two-minute and six-minute ischemia groups at each time point, and for the normal control group. For the sham-operated controls, a single RNA sample was evaluated at each time point. The resultant data was transferred to a database (Filemaker Pro 5, FileMaker, Inc., Santa Clara, CA, USA) and linked to Internet genome databases. To select genes with altered expression patterns, each data array obtained after ischemia was compared with those from the normal, time-matched, sham controls. The criterion of two-fold changes in the average difference for each probe set was used. To further increase the reproducibility, both duplicate samples must have met the two-fold change criteria for the data to be considered. The resultant data was transferred to GeneSpring 4.2 (SiliconGenetics, Redwood City, CA, USA) for hierarchical cluster analysis (Eisen et al., 1998). The most recent information for each transcript was obtained from databases such as Genbank, dbEST, Unigene, and the functional annotation was supplemented by protein database Swiss-Prot.

In Situ Hybridization

Five genes (Egr-2, TIEG, Homer-1C, BTG2, Caspase-2) that showed increased expression levels were chosen for this experiment. Total RNA obtained from normal adult rat brain, as described above, was subjected to RT–PCR using Ready-To-Go T-Primed First-Strand Kit (Amersham Biosciences, Buckinghamshire, UK) and Amplitaq Gold (Applied Biosystems, Foster City, CA, USA) according to the manufacturer's protocols. Sense and antisense PCR primers (22mers) were designed to amplify a fragment of Egr-2 (Accession No: U78102, 1821–2351, 531bp), TIEG (Accession No: U88630, 358–807, 450bp), Homer-1C (Accession No: AF030088, 1852–2332, 480bp), BTG2 (Accession No: M60921, 1861–2294, 434bp), and Caspase-2 (Accession No: U77933, 1641–2163, 470bp). PCR was conducted for 43 cycles (94°C for 30 seconds, 60°C for one minute, 72°C for one minute), and the obtained PCR fragments were subcloned into pPCR-Script Amp SK(+) (Stratagene, La Jolla, CA, USA). Orientation and sequence were verified by direct sequencing. Antisense and sense RNA probes were prepared from each cDNA using RNA labeling kit (Riboprobe Combination System-T3/T7, Promega, Madison, WI, USA) with T7 and T3 RNA polymerases. The probes were labeled by [α-^{35}S]-UTP (Amersham Biosciences) to a specific activity of approximately 1–2 × 10^6 cpm/ng.

The animals were sacrificed 1, 3, 12, 24, and 48 hours after ischemia under deep anesthesia with 4% halothane, the brains were immediately removed, frozen in powdered dry ice, and cut into 14 μm-thick coronal sections approximately 3.8 mm from bregma (Paxinos and Watson 1986) using a cryostat at −16°C. *In situ* hybridization was performed as previously described (Kawahara et al., 1999). Briefly, sections postfixed with 4% paraformaldehyde were hybridized with each cRNA probe at 55°C for 16 hours at a concentration of 1.0×10^4 cpm/μl. The next day, high stringency washes at 55°C were followed by RNase A treatment and dehydration. The sections were exposed, with a radioactive standard strip, to BioMax MR film (Eastman Kodak, Rochester, NY, USA) for 3–7 days.

RESULTS

Delayed Neuronal Death and Induction of Tolerance

In the first experiment, ischemic neuronal injury in the hippocampal CA1 sector was examined (Fig. 1). The CA1 neurons were significantly reduced only in the six-minute ischemia group (9.7 ±2.9% of normal control, $p<0.0001$ by ANOVA, with Bonferroni's post-hoc test) compared with those in the sham (90.3 ±6.8%) and two-minute (91.3 ±12.6%) groups. This observation indicates that, in our rat global ischemia model, six-minute ischemia is sufficient to induce severe hippocampal neuronal death, whereas two-minute ischemia does not cause any detectable injury. In the double ischemia experiment (Fig. 1), rats were subjected to either sham operation or two-minute ischemia three days prior to six-minute ischemia, and then sacrificed seven days later. Evaluation of hippocampal neuronal injury demonstrated that preconditioning via two-minute ischemia significantly protected CA1 neurons against subsequent six-minute ischemia (27.2 ±17.5% in sham and 80.6 ±8.8% with two-minute preconditioning, $p<0.0001$ by unpaired t-test), which confirmed the belief that short sublethal ischemia, provided by two-minute ischemia in our model, induced ischemic tolerance at three days.

Global Changes in mRNA Expression following Ischemia

Of 8,799 probe sets represented on the chip, 3,518 transcripts (40%) were considered present in normal controls according to the manufacturer's default computer algorithm. Of these, 238 transcripts, which correspond to 2.7% of the total probe set, were increased after ischemia compared with normal and time-matched sham controls using our current criteria (Fig. 2). In this group, 36 transcripts were increased following two-minute ischemia, and 224 transcripts following six-minute ischemia, while 22 transcripts were increased in both conditions. Similar analysis for decreased expression showed that 205 transcripts were down regulated following ischemia (2.3% of the total probe set), which was similar to the number of increased expression. Eight transcripts showed both up and down-regulation during their time course, giving a total of 451 transcripts (5.1% of the total probe set) that exhibited significant changes following ischemia. These were subjected to further analysis.

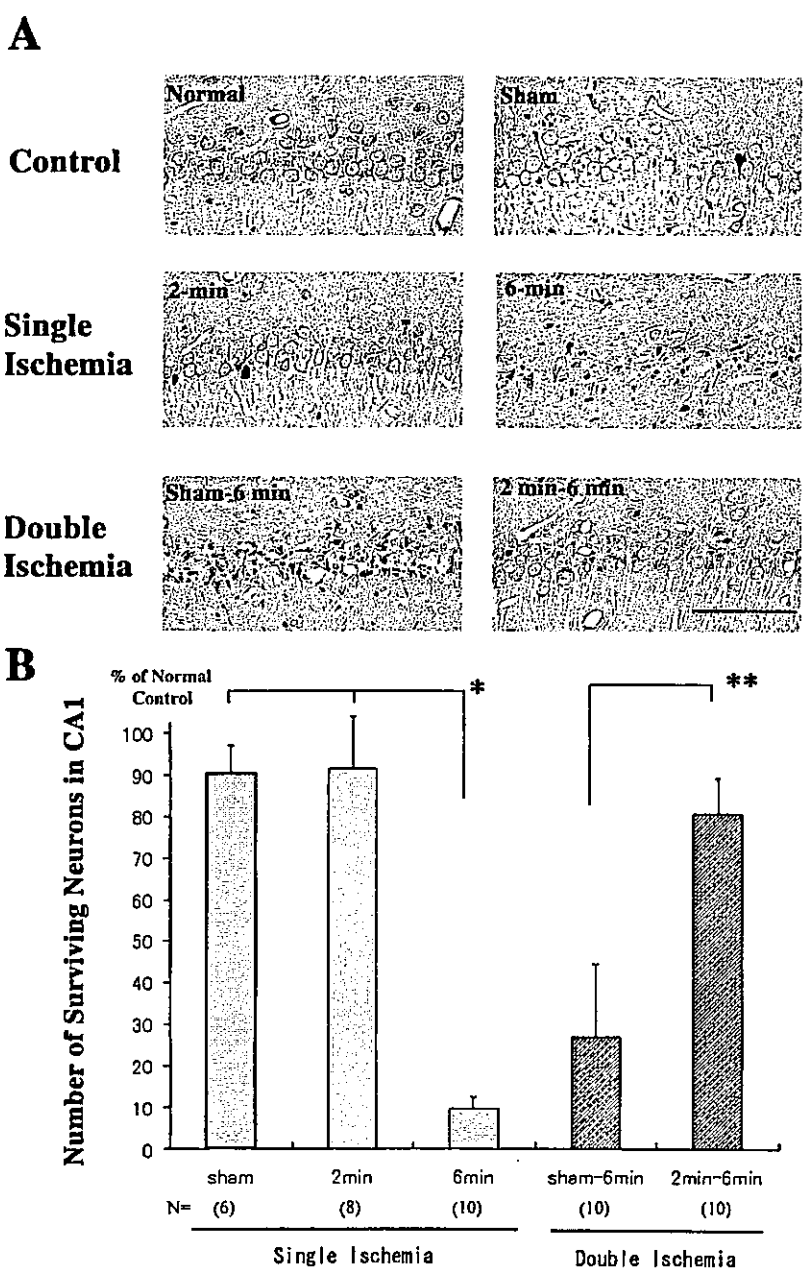

FIG. 1. A. Histological outcome in the CA1 sector of the hippocampus after single (two- and six-minute) and double (sham and six-minute, two- and six-minute) ischemia. Single short ischemia (two-minute) did not cause significant cell injury, while longer six-minute ischemia led to uniform severe neuronal death. Prior pretreatment with two-minute ischemia remarkably protected pyramidal neurons against otherwise lethal six-minute ischemia. Hematoxylin and eosin staining. Scale bar: 100 μm. B: Bar graph showing the density of intact neurons in the CA1 sector in each group, presented as % of normal control (mean ±SD).

Hierarchical Cluster Analysis for Coordinated Changes in mRNA Expression

To analyze the patterns of coordinated mRNA expression, we applied hierarchical cluster analysis (Eisen et al., 1998) to the transcripts with altered expression levels and could categorize these into seven clusters. As shown in Fig. 3, each cluster displayed distinctive time- and condition-specific characteristics. Transcripts included in cluster 2 showed immediate transient increases after both two- and six-minute ischemia, and corresponded to the majority of the up-regulated genes in two-minute ischemia, which overlap with a subset of those in six-minute ischemia. Specific changes in six-minute ischemia were shown in clusters 1 and 7, where these transcripts exhibited delayed increase or decrease, respectively. The transcripts in cluster 4 were markedly increased solely after six-minute ischemia. To analyze what type of transcripts are in each expression cluster, we searched nucleic acid databases, deleted duplicate transcripts of the same gene, and grouped each transcript into 20 functional categories. However, we could not find specific functional groups in the majority of clusters (data not shown), except clusters 2 and 4, which were highly specific for signal transducers/transcription factors and heat shock proteins, respectively.

Comparison of mRNA Expression between Ischemic Tolerance and Neuronal Death

To analyze differential expression profiles between two- and six-minute ischemia, genes with altered levels

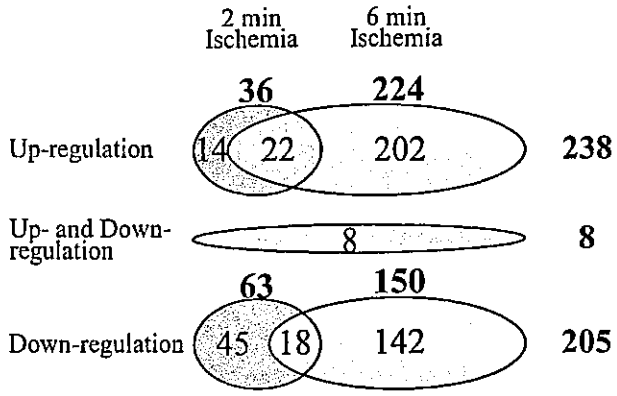

FIG. 2. Diagram showing the number of gene transcripts, up or down-regulated, after either two- or six-minute ischemia. Changes after two-minute ischemia are depicted in blue, those after six-minute in yellow, and those with overlapping transcripts in green. The transcripts showing both up and down-regulation during their time course are included in a separate circle in red.

of expression were compared according to their functional categories. The main results are shown in Fig. 4; some of the individual genes are listed in the Table and Fig. 5. The complete data set for individual transcripts is available at our web site (http://www2.genome.rcast.u-tokyo.ac.jp/egl/index_e.html).

Following two-minute ischemia, the majority of up-regulated genes are transcription factors, signal transducers, receptors, heat shock proteins, and cell cycle proteins. Among the transcription factors, leucine zipper transcription factors (c-Fos, JunB), zinc finger Egr family members, such as Egr-1 (NGFI-A, Krox24, zif268), Egr-2, Egr-4 (NGFI-C), and the closely related nuclear orphan receptor NGFI-B (Nurr77), showed increased expression. A marked up-regulation of mitogen-activated protein kinase phosphatases (MKP-1 and -3) was observed. In particular, MKP-1 showed a 10-fold increase in gene expression after two-minute ischemia. With regard to heat shock proteins, only HSP70 was up-regulated.

Following six-minute ischemia, several distinctive features were noted compared with those in two-minute ischemia, although similar up-regulation within the same functional categories was observed. Transcription factors related to cell death and growth arrest (KLF4, RNF4, GADD153, Smad2, NFκ b), signal transducers for cyclic AMP signaling (CAP1, PKI, ARPP-12, PDE4A), and proapoptotic factors (Dral, Caspase 2 and 3) were specifically increased after six-minute ischemia. Secondly, various heat shock proteins were increased, such as Hsp60, Hsp40, Hsp32, Hsp27, in addition to Hsp70. Finally, a substantial number of genes belonging to various functional groups were down-regulated. Of particular interest among these are signal transducers related to MAP kinase pathways (MKK2) and phosphatidyl inositol signaling (PI3 kinase, PI4 kinase), diacylglycerols (diacylglycerol kinase-2, -3, -6), protein kinase C (PKC β and γ), calcium/calmodulin dependent protein kinase (CAMK II α and β) and calcium signaling (IP3 kinase, IP3 receptor). In addition to these, glutamate receptors of various types, such as AMPA-type (GluR-1, -2, -3), NMDA-type (NMDAR1, NMDAR2A), and metabotropic type (mGluR3), were also down-regulated, as well as TGF beta receptor.

In Situ Hybridization

To confirm the microarray data, we selected five genes from four different categories that showed increased expression and performed *in situ* hybridization study. For each gene, the autoradiographs at the peak value in the microarray experiment are shown in Fig. 6. Egr-2 (a transcription factor), TIEG (TGF inducible early growth response protein), and Homer-1C (a postsynaptic membrane protein) showed early increase in both two- and six-minute ischemia in the microarray experiment. These increases were confirmed in the CA1 pyramidal layer by *in situ* hybridization for Egr-2 and Homer-1C. However, the hybridization signal in TIEG was equivocal. BTG2 (B-cell translocation gene 2) and Caspase-2 showed increased expression only after six-minute ischemia, which were also confirmed by *in situ* hybridization. Thus, time-course and condition-specific alterations of mRNA expression were confirmed for four out of five genes.

DISCUSSION

We used a nonbiased oligonucleotide-based DNA microarray to assess alterations in gene expression after ischemia in the hippocampal CA1 region, where ischemic cell death and tolerance are specifically demonstrated. Of a total of 8,799 transcripts surveyed, 3,518 transcripts (40.0%) were present in normal conditions and 451 (5.1%) exhibited distinct changes following ischemia. Among these, ischemic tolerance was associated with changes in only 1.2% of the total transcripts, whereas ischemic cell death induced changes in 4.5%. This ratio is consistent with other studies which demonstrated changes in 0.6–2.0% of genes screened in physiological conditions such as aging (Lee et al., 2000) and environmental enrichment (Rampon et al., 2000), while pathological conditions were associated with a greater number of changes ranging from 6 to 10% (Friddle et al., 2000; Song et al., 2001; Stanton et al., 2000). In this regard, our study confirmed the idea that cellular injury is associated with greater changes in gene expression when compared with those in cellular adaptation to the same insult, in our case, ischemia.

A major obstacle in expression profiling by DNA microarray technology has been how to analyze a huge data set to obtain indicative information underlying a specific condition. We used hierarchical cluster analysis, which can efficiently group together the transcripts with similar

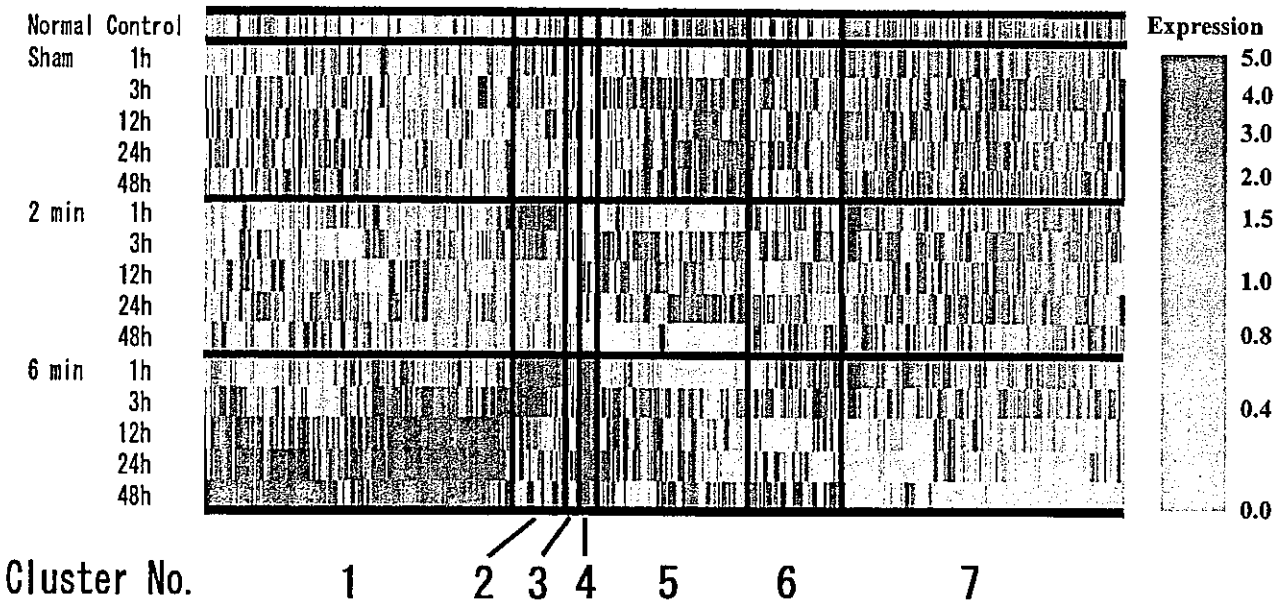

FIG. 3. Clustered gene expression patterns of 451 transcripts that displayed differential expression in two- or six-minute ischemia by hierarchical cluster analysis. Each column represents an individual transcript and the row pertains to different data sets collected at different conditions and times as indicated. Genes with similar patterns of changes were grouped into seven clusters with distinct time and condition-specific features.

changes by pairwise, average-linkage cluster analysis (Eisen et al., 1998). This approach revealed condition-specific changes, for example, that six-minute ischemia induced delayed and long-lasting changes compared with two-minute ischemia, as demonstrated by clusters 1 and 7. This clearly indicates that lethal ischemia initiates more complex, long-lasting cascades of molecular events. Although this approach is expected to produce similar functional groups (Lockhart and Winzeler 2000), we did not observe specific correlation, except for

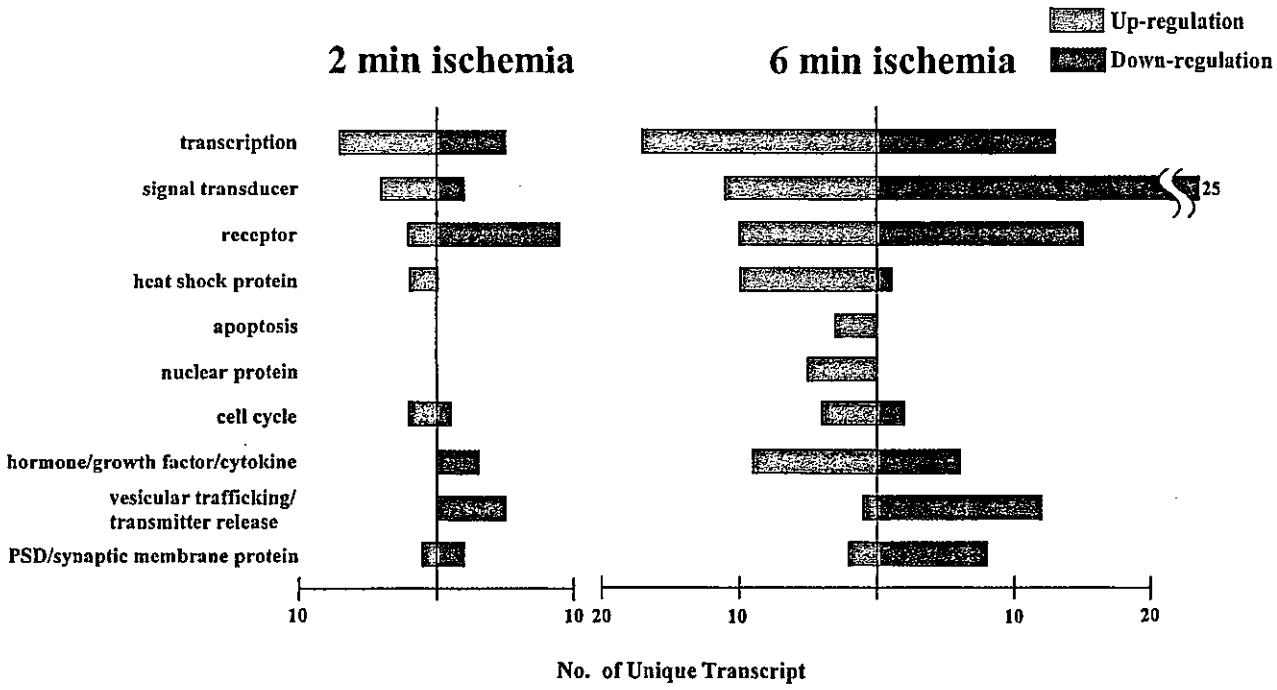

FIG. 4. Bar diagram showing the numbers of transcripts in 10 major functional categories that exhibited up and down-regulation after two- and six-minute ischemia. Some categories, such as transcription, signal transducer, and heat shock proteins exhibited similar patterns, whereas apoptosis proteins, nuclear proteins, and hormone/growth factor/cytokine groups were more specifically altered after six-minute ischemia.

TABLE 1. *List of genes in relation to ischemia*

Genbank accession no	Gene name	Normal control	Peak changes (fold)				Cluster no
		Average signal	2 minutes		6 minutes		
			Increase	Decrease	Increase	Decrease	
Transcription							
X06769	c-fos	20	7.70		17.26		2
U78102	EGR-2 (KROX20)	31	4.84		7.45		2
X54686	Jun-B	34	3.44		4.38		2
AI172476	TGF-beta inducible early growth response (Tieg)	39	2.78		5.37		1
U75397	EGR-1 (NGFI-A, KROX24)	410	2.66		3.29	0.32	7
M92433	EGR-4 (NGFI-C)	141	2.61		3.33		2
U17254	NGFI-B (Nurr77)	271	2.13		2.19		7
L26292	Kruppel-like factor 4 (KLF4)	20			7.19		2
AF022081	Ring finger protein 4 (RNF4), SNURF	21			3.85		5
U30186	GADD153	27			2.95		1
AB017912	Smad 2	30			2.55		1
L26267	NF kappa b p105 subunit	35			2.24		1
Signal transducer							
U02553	MAP kinase phosphatase 1(MKP-1)	20	10.58		14.14		2
X94185	MAP kinase phosphatase 3 (MKP-3)	165	2.30	0.23	2.97		2
L11930	Adenylyl cyclase-associated protein 1(CAP1)	119		0.44			1
L02615	cAMP-dependent protein kinase inhibitor (PKI)	26			3.29		1
S65091	cAMP-regulated phosphoprotein, ARPP-21	32			2.55		1
M26715	cAMP-dependent phosphodiesterase (PDE4A)	50			2.35	0.40	7
L14936	MAP kinase kinase (MKK2)	152				0.21	5
X07287	PKC gamma	443				0.21	7
X56917	IP3 3-kinase	596				0.25	7
U38812	IP3 receptor	67				0.30	7
M16960	CAMK II, alpha chain	86				0.31	7
D832538	PI 4-kinase, 230kDa	91				0.33	7
AA818983	Diacylglycerol kinase-2	52				0.38	5
D38448	Diacylglycerol kinase-3	84				0.39	7
D64046	PI3-kinase p85 beta subunit	61				0.39	7
K03486	PKC beta	413				0.40	7
M16112	CAMK II, beta chain	1269				0.41	7
D78588	Diacylglycerol kinase-6	1090				0.48	7
Receptor							
M36419	Glutamate receptor (GluR-2)	347		0.27			5
M92076	Metabotropic glutamate receptor 3 (mGluR-3)	385		0.35			5
M36420	Glutamate receptor (GluR-3)	45		0.45		0.45	5
M77809	TGF-beta receptor type 3	104				0.19	7
M36418	Glutamate receptor (GluR-1)	161				0.22	7
U11418	Glutamate receptor (NMDAR1)	86				0.32	7
AF001423	Glutamate receptor (NMDAR2A)	47				0.43	7
Heat shock protein							
Z75029	Heat shock protein 70	20	10.48		133.88		4
AA998683	Heat shock protein 27	21			71.64		1
U68562	Heat shock protein 60	133			8.38		1
AI170613	Heat shock protein 10	322			5.13		1
AA800551	Heat shock protein 40 (DnaJ-like protein)	345			4.08		1
AI179610	Heat shock protein 32 (heme oxygenase)	52			3.93		1
Apoptosis							
U77933	Caspase 3	20			2.99		1
U49930	Caspase 3	21			2.66		1
AA891527	Dral	161			2.28		1
Cell cycle							
AF030091	cyclin ania-6a	23	5.49		6.39		1
D14014	Cyclin D1	20	3.46				5
M60921	B-cell translocation gene 2 (BTG2)	30			5.43		2
PSD, synaptic membrane protien, vesicular trafficking/transmitter release							
AF030088	Homer-1C (PSD-ZIP45)	29	2.97		11.51		2

clusters 2 and 4 which were mostly specific to signal transducer/transcription factors and heat shock proteins, suggesting limitation of this assumption in ischemia.

One of the main purposes of our study was to find key molecular events leading to ischemic tolerance and delayed neuronal death by global expression monitoring. This approach is based on the hypothesis that the abundance of RNA is proportional to the amount of protein. After lethal ischemia, it is known that translational activity is significantly decreased (Kleihues and Hossmann

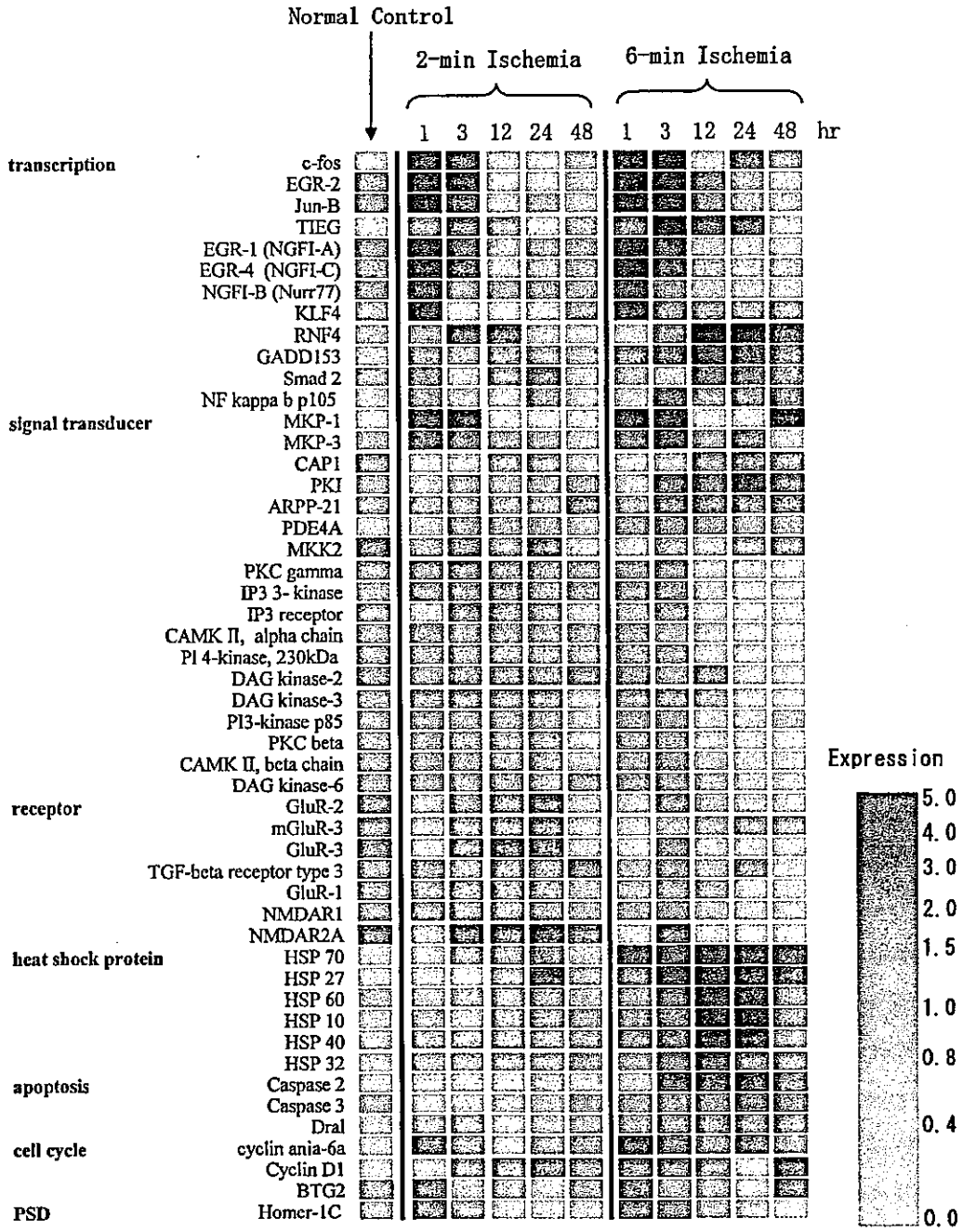

FIG. 5. Expression levels of a subset of genes described in Table. These genes are categorized into functional clusters and their expression levels are shown by color for comparison among normal control, two-minute and six-minute ischemia with time course.

1971). Thus, ischemic tolerance induced by sublethal ischemia is a suitable model for this approach, since it has been shown to be dependent on *de novo* protein synthesis (Barone et al., 1998). The most conspicuous changes we observed were for HSP70, leucine zipper and zinc finger transcription factors, such as c-Fos, JunB, Egr-1 (NGFI-A, Korx-24), Egr-2 (Krox-20), Egr-4 (NGFI-C), and a DNA-binding nuclear orphan receptor NGFI-B (Nurr77), which are regulated by a variety of stimuli or insults (for review, refer to Herdegen and Leah, 1998). Fos and Jun family members are implicated in neuronal degeneration following ischemia. In particular, c-Jun and JunB induction is observed in dying neurons after ischemia (Dragunow et al., 1994; Whitfield et al., 1999). Recently, a peptide inhibitor for c-Jun N-terminal kinase (JNK) that phosphorylates c-Jun has been shown to dramatically reduce infarction, which was accompanied by c-Jun activation and c-Fos transcription, thus indicating a critical role for AP-1 binding proteins in ischemic injury (Borsello et al., 2003). However, contra-

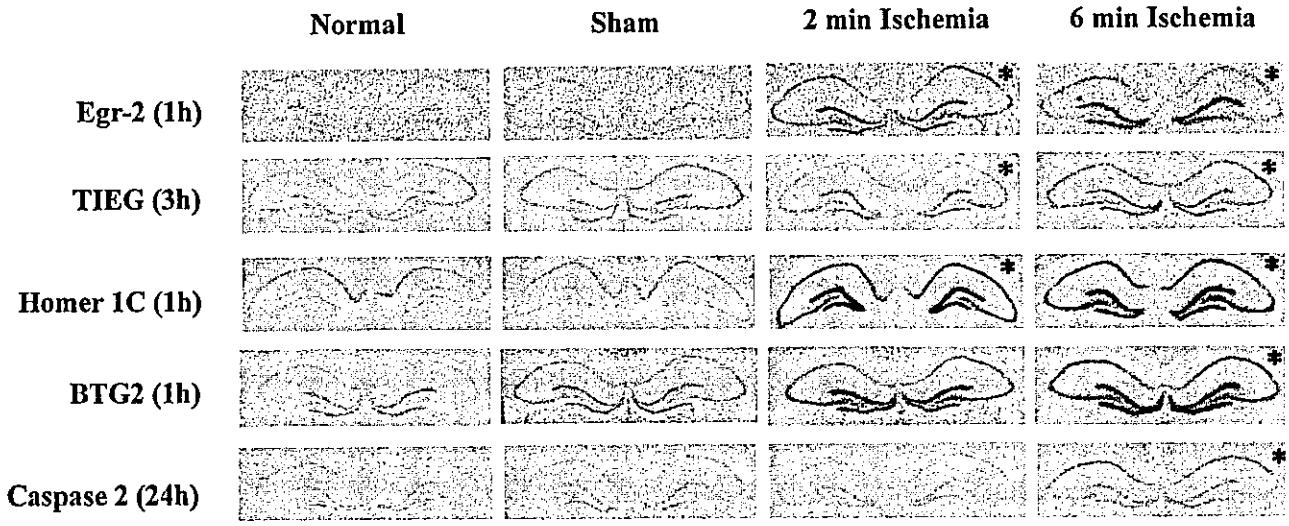

FIG. 6. *In situ* hybridization autoradiogram for Egr-2, TIEG, Homer-1C, BTG2, Caspase-2. The time-points and conditions that showed increased expression by the microarray analysis were indicated by the asterisks on the autoradiograms. Comparison between these independent methods disclosed corresponding results in four out of five genes, though the signal intensity on the CA1 sector following ischemia was equivocal for TIEG.

dictory observations have been reported that mRNA for c-Fos and JunB were widely expressed in the surviving peri-infarct area after focal ischemia (Kinouchi et al., 1994). Consistent with our observations, c-Fos and c-Jun have been shown to be up-regulated in sublethal ischemia (Sommer et al., 1995; Truettner et al., 2002) and spreading depression (Kariko et al., 1998), that renders brain resistant to ischemic injury (Kawahara et al., 1995; Kirino et al., 1991). Furthermore, hypothermia (Akaji et al., 2003) and treatment with a neuroprotective agent (Cho et al., 2001) during ischemia increased expression of c-Fos, while its attenuation by antisense oligonucleotide led to increased ischemic injury (Zhang et al., 1999). Since it is known that c-Fos and c-Jun heterodimerizations decrease the transcriptional activity of c-Jun (Herdegen and Leah, 1998), the increase in c-Fos expression may attenuate c-Jun signaling cascade to favor neuronal survival. Considering these opposing results, the effect of complex AP-1 binding protein signaling on cerebral ischemia needs to be clarified by further study.

Similarly, roles of zinc finger-transcription factors in cerebral ischemia are still controversial. For example, Egr-1 (NGFI-A, Korx-24), Egr-2 (Krox-20), Egr-4 (NGFI-C), and NGFI-B (Nurr77) were induced following focal and global ischemia (Honkaniemi and Sharp 1996; Honkaniemi et al., 1997), in which persistent expression of Egr-1 was associated with delayed neuronal death in CA1. Egr-1 and NGFI-B have been shown to induce apoptotic cell death in various *in vitro* studies (Catania et al., 1999; Li et al., 2000). However, *in vivo* evidence for a proapoptotic role in cerebral ischemia is still lacking. On the contrary, Egr-1 up-regulates the expression of antioxidant (Maehara et al., 2001) and neuroprotective EGF receptor (Nishi et al., 2002), and has been found to inhibit apoptosis following ultraviolet irradiation (Huang et al., 1998). NGFI-B has also been found to inhibit apoptosis when phosphorylated by Akt (Masuyama et al., 2001). Consistent with our findings, these observations may suggest a neuroprotective role in several contexts of insult such as sublethal ischemia.

Another important change in ischemic tolerance was robust up-regulation of MAP kinase phosphatase 1 and 3 (MKP-1 and -3). These phosphatases dephosphorylate and inactivate proteins of the mitogen activated protein kinases (MAPK) cascades (Franklin and Kraft 1997; Zhao and Zhang 2001), such as ERK (extracellular-signal regulated kinase), JNK, and p38 which play crucial roles in various stress conditions (for review, refer to Irving and Bamford, 2002). During cerebral ischemia, JNK and p38 are immediately phosphorylated (activated) and considered detrimental signals for neuronal death (Borsello et al., 2003; Gu et al., 2000; Sugino et al., 2000). Though ERK is also activated after lethal ischemia (Namura et al., 2001), its role is still controversial because it has been recently shown to be a critical pathway for induction of ischemic tolerance *in vitro* (Gonzalez-Zulueta et al., 2000), as well as *in vivo* (Gu et al., 2000; Gu et al., 2001). Of particular interest is the observation that MKP-1 is transcriptionally up-regulated and phosphorylated by ERK, leading to stabilization of the protein (Brondello et al., 1997; Brondello et al., 1999). MKP-1 is also up-regulated by hypoxia (Bernaudin et al., 2002), spreading depression, and in the peri-infarct region, which are not accompanied by neuronal injury (Gu et al., 2000; Hermann et al., 1999; Irving and Bamford 2002; Soriano et al., 2000). Since its higher

phosphatase activity is shown against JNK and p38 compared to that against ERK (Franklin and Kraft 1997), it acts rather specifically as an inhibitor of JNK and p38 signaling. Based on these findings, we speculate that MKP-1 induced by sublethal ischemia may "prime" the neurons to inhibit detrimental signals through JNK and p38 during subsequent lethal ischemic insult thus contributing to ischemic tolerance. Though this hypothesis seems attractive, it has to be verified by further *in vitro* and *in vivo* experiments at the protein level.

Compared to ischemic tolerance, remarkable changes in gene expression were associated with delayed neuronal death. However, these changes should be cautiously interpreted when considering the general translational inhibition after long lethal ischemia (Kleihues and Hossmann 1971). Nevertheless, several unique features of our study should be mentioned since some proapoptotic gene products are still increased in this condition, such as Bax and Caspase-3 (Chen et al., 1996; Chen et al., 1998), in addition to the well-described up-regulation of various heat shock proteins (Abe et al., 1998). Firstly, a substantial number of genes implicated in cell death were increased, such as NF κ b (Schneider et al., 1999), KLF4 (Chen et al., 2000), RNF4 (Pero et al., 2001), GADD153 (Murphy et al., 2001), and TGF signaling DNA biding protein Smad2 (Jang et al., 2002). Similarly, proapoptotic factors such as Caspase-2 and 3, and Dral were also increased. Caspase-2 and 3 are proteases that mediate apoptotic signals, and have already been implicated in ischemic neuronal death (Chen et al., 1998; Jin et al., 2002), whereas Dral is a newly identified gene that is p53 responsive and implicated in apoptosis (Scholl et al., 2000). Secondly, a large number of genes were down regulated. Of particular interest among these are signal transducers involved in ERK (MKK2), PI3 (PI3 kinase, PI4 kinase), and DAG/PKC (diacylglycerol kinase-2, 3, 6, PKC β and γ) pathways. Although the roles of these pathways in cell death or survival are controversial, several studies have shown their critical role as survival factors (Gu et al., 2001; Maher 2001; Marte and Downward 1997; Xia et al., 1995), which may imply attenuation of survival signals in ischemic neuronal death. PI4 kinase, a key enzyme in growth promoting PI3 kinase-Akt/PKB pathway (Marte and Downward 1997), has been shown independently to be down-regulated in ischemic neuronal death, and demonstrated to be neuroprotective when expressed persistently (Furuta et al., 2003). These observations would indicate an overall transcriptional response leading to an imbalance between death and survival signals in ischemic neuronal death, a distinctive feature not observed in ischemic tolerance.

Finally, a critical issue inherent in the current study is whether the data is reliable. We first evaluated reproducibility of housekeeping genes (GAPDH and β actin) among different arrays and confirmed that differences of expressions are within two-fold changes (data not shown). We next set the filtering value of two-fold change for duplicate samples, since this cutoff value has already been used and validated in non-tumorous expression analysis (Jin et al., 2001; Stanton et al., 2000). Another method of validation is to compare our results with those already reported in microarray analysis after ischemia (Bernaudin et al., 2002; Jin et al., 2001; Keyvani et al., 2002; Soriano et al., 2000). However, due to the differences in the model, the sampling region and timing, direct comparison is difficult. Instead, we conducted a literature search for 311 annotated genes listed in our study and identified 135 genes (43%) whose changes in expression have previously been described following ischemia in various tissues. In addition, we conducted an independent study by *in situ* hybridization, which revealed corresponding results in four out of five genes examined. However, some genes already described to be up-regulated in global ischemia did not appear in our profile, such as Bax (Chen et al., 1996). Bax transcripts exceeded the two-fold cutoff value only once in our experiments, thus failing to meet our current criteria. Though this observation may suggest low sensitivity (higher false negative rate), our results for ischemia seem to provide more specific data (lower false positive rate). Other studies also supported the reliability of oligonucleotide microarray data when compared with other validation methods, such as RT-PCR (Bernaudin et al., 2002; Tang et al., 2001), and others (Chudin et al., 2002; Ishii et al., 2000). New methods for microarray data analysis are being developed to improve sensitivity and specificity in a variety of experimental paradigms, such as Significance Analysis of Microarray Data (SAM) and Expression Deconvolution Analysis (Lu et al., 2003; Tusher et al., 2001). Further improvements and application of these methods to complex data, such as expression profiling of multiple groups along a time course, as in the current study, would improve data mining. Reinterpretation of the raw data derived from various ischemia related studies will be required in the future, using these highly sophisticated methods.

Our study revealed a wide variety of transcriptional responses with distinct patterns in relation to two different ischemic insults, namely delayed neuronal death and induced tolerance in the hippocampal CA1 region. Induced tolerance was associated with immediate and transient responses in a limited number of genes, whereas neuronal death was accompanied by immediate responses followed by delayed and long-lasting changes in a larger number of genes. Combined with changes in each gene, this genome-wide view of genomic responses will deepen our understanding of cerebral ischemia by narrowing our focus to target pathways or molecules and contribute to clarification of the molecular pathophysiology of delayed neuronal death and ischemic tolerance.